Particle-driven gravity currents

Part 2: Experimental results

Master of Science Thesis

For obtaining the degree of Master of Science in Offshore and Dredging Engineering at Delft University of Technology

Obaid Abrahimi

August 31, 2021

Particle-driven gravity currents

Author:
O. Abrahimi BSc, 4124936

Thesis Committee:
Prof. Dr. Ir. C. van Rhee
Dr. Ir. J.C. Goeree [TU Delft / Royal IHC]
Dr. Ir. A.M. Talmon

TU Delft
Delft University of Technology

Abstract

Particle-driven gravity currents cause major geological problems. Turbidity currents are highly erosive and can be damaging to structures on the sea bottom such as telecommunication cables. Understanding the mechanisms of sediment transport and deposition is required to predict the erosive powers of turbidity currents (and of the distribution of turbidite deposits) which are fully dependent on the behavior of gravity currents. For this reason, the main question of this thesis was formulated: Which physical parameters of the gravity current are of importance for its behaviour?

The lock-exchange release experiment is a frequently used method to study gravity currents in a laboratory and was also used in this thesis. In order to answer the main question, the following parameters were investigated and their influence specifically on the 4 phases, the run-out length and the PSD: particle size, bed roughness and temperature. The influence of particles size was researched using mono-dispersed vs bi-dispersed experiments. In the bed roughness experiments, sandpaper was attached to the bottom and compared to smooth bed experiments. Finally, to investigate the influence of temperature on the gravity current, experiments with warm water were compared to experiments with colder water.

From these experiments, the most notable results are summarized below.

PSD: For all experiments applies that at low concentration the particles segregate over the run-out length of the gravity current. Smaller particles travelled further than the bigger particles with a higher settling velocity. This does not occur at higher concentrations and the PSD over the entire run-out length is similar.

Four Phases: In all experiments, the four phases could clearly be identified with one exception: the first phase in the rough bed experiments was difficult to distinguish.

Run out length: Some interesting findings were made that were in line with literature: adding fine particles to the mixture of the current cause the run-out length of the current to increase. However, it was also found that if the initial concentration is increased, this effect decreases. Furthermore experiments showed that an increase in temperature can cause the current to travel less far when compared to experiments performed with water with lower temperature.

In the light of this research, the following recommendation are made: Temperature should be taken into account for modelling gravity currents. Otherwise this can lead to an overestimation regarding the run-out length and an underestimation of the deposit density. Furthermore, to get more insight in the effect of the particle sizes in the currents, it would be highly recommended to conduct more experiments with a greater difference between particle sizes. This would allow for a better assessment of the magnitude of the effect of hindered settling

Obaid Abrahimi
Rotterdam, 2021

Table of contents

List of Figures

List of Tables

List of Symbols

γ	Light over heavy density ratio ρ_1/ρ_2 [-]
μ	Dynamic viscosity [kg/(m·s)]
ν	Kinematic viscosity [m/s^2]
ϕ	Volume fraction of particles [-]
ϕ_0	Volume fraction of particles in suspension at $t_0[-]$
ρ_a	Density ambient fluid[kg/m^3]
ρ_c	Density of the current[kg/m^3]
σ	Normal stress component[N/m^2]
τ	Shear stress component [N/m^2]
A_0	Surface area of the bottom behind the lock gate [m^2]
C_d	Drag coefficient [-]
d	Particle diameter [m]
d_{50}	Median grain size [m]
F	Force [N]
Fr	Froude number [-]
g	Gravitational acceleration [m/s^2]
g'	Reduced gravity [m/s^2]
H	Height of the surrounding fluid [m]
h	Height of the gravity current[m]
L	Length of the tank [m]
l	Position of the front in the channel [m]
M	Mass of particles added to the suspension [kg]
n_m	Manning friction coefficient [s/m$^{1/3}$]
p	Pressure [kg/(m s^2)]
p_0	Atmospheric pressure [kg/(m s^2)]
Re	Reynolds number [-]
T	Stress deviator tensor [-]
t	Time [s]
u	Velocity in x-direction [m/s]
v_0	Terminal settling velocity of a single particle [m/s]
v_f	Fluid velocity [m/s]
v_p	Particle velocity [m/s]
v_r	Relative velocity [m/s]
v_s	Particle settling velocity [m/s]
W	Width of the channel [m]
x	Horizontal coordinate[m]
x_0	Position of the lock-gate [m]

Chapter 1

Introduction

In the first part of the thesis, a general introduction is given on gravity currents and its importance is addressed. Additionally, an overview of important literature is given on this subject. Furthermore, the key question and sub-questions are stated and further outlined. The numerical model is introduced.

The research question is:

Which physical parameters of the gravity current are of importance for it's behaviour and can the numerical model simulate a gravity current correctly with varying physical parameters?

The sub-questions are formulated as:

1. What is the influence of particle size(s) of the mixture for the behaviour of a gravity current?
2. What is the influence of bed roughness on the behaviour of a gravity current?
3. What is the influence of temperature of the mixture for the behaviour of a gravity current?

This (second) part of the thesis is an extension of the first part and presents the results of the lab experiments. The results are set side by side to the literature and the questions stated above are answered based on the results and comparison with the literature.

1.1 Outline

After this brief introduction chapter, chapter 2 of this thesis gives more insight in some specific literature and the outline of the key question and sub-questions. Also the experimental methodology used for this thesis is explained, which mainly involves the lab experiments and their set up. Also the difficulties during the process are addressed.

In chapter 3, the results of the experiments are outlined. These experiments are divided over three sections, starting with results of the mono-mix experiments. These experiments are performed in order to identify the influence of the particle sizes in the movement and development of the gravity currents. Secondly, the results of the experiments concerning bed-roughness are presented. The relation between bed-roughness and gravity currents are not researched extensively. Using experiments and the numerical model more insight is gained about this relation. Finally, the experimental results regarding the influence of temperature on gravity currents are presented.

In chapter 4 the results of the numerical model are presented. The results, consisting of multiple simulations, are in line with the experiments presented in chapter 3. The simulations include a range of input parameters for particle size, bed-roughness and temperature similar to the lab experiments. The results of the simulations are compared to each other and discussed.

Finally, in chapter 5 the comparison between the lab experiments and the numerical simulations is made. Conclusions are drawn based on the results given in chapter three and four. Also, recommendations are made based on the results and conclusions.

Chapter 2

Experiments

In addition to the theory comprises the calculations of gravity currents, a literature study is performed in this chapter in order to identify the former studies concerning the three experiments.

2.1 Theory and literature studies

The literature study comprises studies of the 4 phases of a gravity current, the influence of mono- and bi-disperse mixtures, the influence of bed roughness and the influence of temperature. The four topics of the literature study are presented in sections 2.1.1, 2.1.2, 2.1.3 and 2.1.4.

2.1.1 4 Phases

A vertical barrier separates two compartments of a horizontal tank, each filled with fluids of different densities. The difference in densities is caused by particles in the fluid one side of the tank. The higher density fluid is initially held back by the barrier. The experiments involve the sudden removal of the barrier (by hand) causing the instantaneous release of the fixed fluids. The more dense fluid flows underneath the less dense fluid because of hydro static pressure differences. At the same time, the less dense fluid flows in the opposing direction over the more dense fluid. Eventually, the flow will disappear after all the particles have settled.

Former research by [Huppert and Simpson, 1980], [Rottman and Simpson, 1983] has established that three phases can be identified in the spreading of a gravity current in a lock exchange experiment: a slumping phase, an inertial phase and finally a viscous phase. However, this thesis is a continuation of the research done by [Stovers, 2016] in which four phases were described. An extra phase was distinguished called the similarity phase. For this reason, four phases will be differentiated within the evolution of the gravity current in the experiments performed and described in this thesis, as the results should be comparable.

The four phases, slumping, inertial, similarity and viscous are described, based on literature [Shin et al., 2004], as followed:

1. The first phase is the slumping phase. This phase starts shortly after the barrier is removed. The denser fluid flows along the bottom of the tank in one direction while the lighter fluid flows on top of the denser fluid in the opposite direction. The current accelerates. (Gravity Current Propagation Up a Valley).

2. When an almost constant speed is reached, the second phase, called the inertial phase, begins. Buoyancy force of intruding fluid is balanced by the inertial force. [Huppert and Simpson, 1980] This phase is typified by an almost constant speed of the gravity current flows.

3. The similarity phase sets in when a bore that is caused by the reflection of the lighter fluid of the back-wall during the slumping phase, travels faster than the gravity current and

eventually overtakes the nose of the current. During this phase, the velocity of the current steeply decreases.[Rottman and Simpson, 1983] This process slows the gravity current down.

4. The final phase is called the viscous phase. In this phase the buoyancy forces of the fluid are balanced by viscous forces. [Huppert and Simpson, 1980] The viscosity causes the front to advance at a still slower rate .The viscous effects begin to overtake the inertial effects [Rottman and Simpson, 1983] and finally the current disappears.

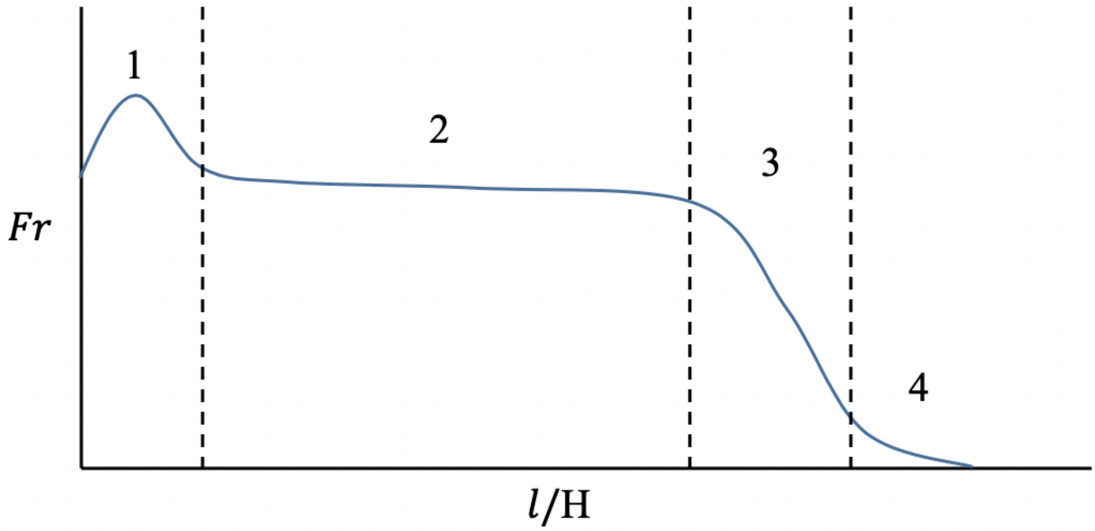

Figure 2.1: Schematic representation of the four phases that a gravity current experiences.

Furthermore, it's worth noting that in [Hallworth and Huppert, 1998], an important observation was made. Beyond a critical initial volume fraction of particles the gravity current underwent an abrupt arrest at some point. According to their data, a value of $\Phi_0 \approx 0.275$ of the initial volume fraction of particles separates two regimes of behavior between currents of different densities (high and low). Currents with initial volume fractions in the range $0.275 < \Phi_0 < 0.45$ underwent an abrupt arrest at some point and as Φ_0 initial concentration increases, the final run out length (of the sediment deposit) decreases. The 0.45 limit is the approximate maximum volume concentration for fluidization. For particle-driven currents within a range of $0 < \Phi_0 < 0.275$ both the run out length and Φ_0 increase.

2.1.2 Mono- and bi-disperse mixtures

To simulate a particle-driven gravity current, a suspension of particles is used as a relatively denser fluid. These suspended particles can either be of the same size or different sizes, also known as mono- or poly-disperse suspensions. Lock-exchange experiments using a mono-and poly-disperse suspensions have been excessively researched [Bonnecaze et al., 1993]. In these experiments, a single average settling velocity was often used for suspended particles. However, it is incorrect to assume that poly-disperse suspensions behave the same way as mono-disperse suspensions. Different particles have different settling velocities. This is an important finding because poly-disperse suspensions are found in natural situations.

When a suspension consists of two different particle sizes, this is called a bi-disperse suspension. Interesting observations have been made in a study by [Dade and Huppert, 1995] and [Gladstone and Woods, 2000]. In a study carried out by [Gladstone and Woods, 2000] all using coarse and fine particles (two grades of silicon carbide with grain sizes 25 μm and 69 μm), it was found that adding coarse particles to a suspension that mostly consisted of fine particles, had little effect on the sedimentation and current evolvement. This is due to the early sedimentation of the coarse particles. However, the opposite turned out to be the case when adding fine particles to the coarse particle suspension. The addition of a small quantity of fine particles, causes the current to travel significantly further than it would without fine particles. The density difference is present for much longer and thus, the current speed does not decelerate as quickly. Fine particles stay in suspension for longer whereas coarse particles sediment early, which explains the greater influence of finer particles. But when coarse particles are accompanied by a small amount of fine particles, the run-out length of the coarse particles is substantially increased.

It is still unknown what the influence is of a greater addition of small particles to a suspension consisting of larger particles. Research has shown that a small amount of small particles has a significant impact on the propagation of the gravity currents final fases[Harris et al., 2001].
A study [Dade and Huppert, 1995] conducted with a bi-disperse suspension established that fine particles prolong and thin the current faster than a mono-disperse suspension with a similar average settling velocity.

2.1.3 Influence of bed roughness

Extensive literature can be found on lock-exchange experiments over smooth beds ([Huppert and Simpson, 1980], [Rottman and Simpson, 1983], [Hallworth et al., 1996],[Zhu et al., 2006]), but research on the dynamics of a gravity current over a rough bed is limited. Also, in the previous work by [Stovers, 2016], the influence of a rough bed has not been measured. One of the aims of this study is to compare the evolution of the gravity current's flow over a smooth bed with the current's flow over a rough bed.

Former research by [Peters and Venart, 2000] on mixing behaviours and flow dynamics of gravity current moving over rough beds, showed that a rough surface retards the front velocity and decreases the concentration of the current's head. Two explanations were given for these effects. To start with, the lighter fluid caught in the roughness layer is driven into the the current causing it to weaken the buoyancy differences between the gravity current and the lighter fluid and as a result the advance velocity over the entire length of the tank is lower. Furthermore, greater shear stress on the bottom of the tank caused by an increased bed roughness also leads to greater flow resistance and viscous effects.

More recently,[La Rocca et al., 2008] investigated the dynamics of three-dimensional gravity currents flowing over smooth surfaces and rough surfaces. The roughness of the bottom surface was varied by gluing a layer of sediment material on the bottom bed using different diameters. The density of the lock fluid was also varied. The following observation was made: a greater diameter of the sediment material on the bottom caused the front velocity to decrease more and earlier than over a smooth bed. This effect was most prominent after the second phase when the velocity starts to decrease, as can be seen in figure 2.1.

2.1.4 Influence of temperature

Gravity currents can be found all over the world. It is important to keep in mind that geological and environmental circumstances vary greatly over the globe. The average ocean surface water is about 17 °C but the world sea temperatures can range from 0 °C to roughly 35 °C depending on the location. The depth of the water should also be taken into account, at deeper sea levels the temperatures decrease. The same is true for lake waters, temperatures can differ from place to place and are also influenced by seasonal changes. With temperature difference the density of the water will change. When the density of water change this will influence the behaviour of the gravity current.

There is also another important factor that has an inverse relationship with water temperature (as mentioned before), the viscosity of the water. This is also relevant for the (laboratory) gravity current. Viscosity is the resistance of a fluid to flow. Cohesive forces between water molecules are the source of viscosity. When the temperature increases, the atomic bonding between the molecules breaks, which leads to a decrease in viscosity, as can be seen in figure 2.2. The water molecules can move freely when this happens.

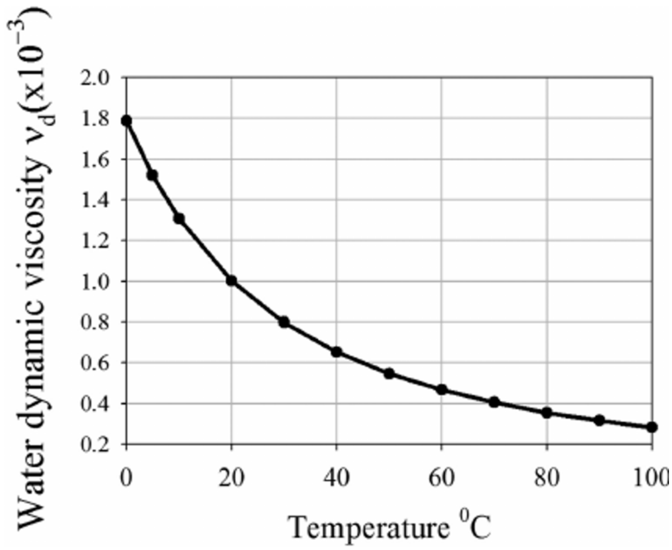

Figure 2.2: Dynamic viscosity as a function of temperature.

Not only temperature has an influence on the viscosity, it is also governed by the particle concentration. [Thomas, 1965] developed an empirical formula to calculate the increase in viscosity as function of the concentration:

$$\frac{\mu_s}{\mu_0} = 1 + 2.5\phi + 10.05\phi^2 + 0.00273e^{16.6\phi} \tag{2.1}$$

The viscosity of the suspension is represented by μ_s, the viscosity of the homogeneous fluid (without particles) by μ_0 and the concentration by the symbol ϕ. A visual representation can be seen in figure 2.3.

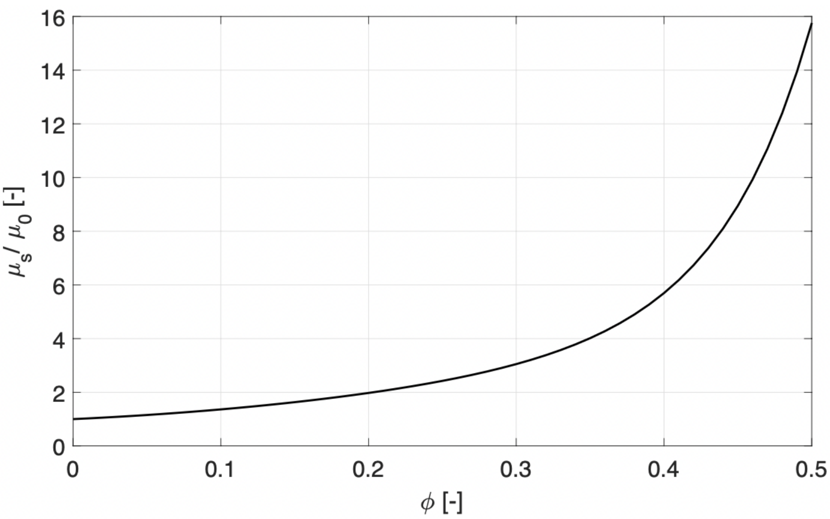

Figure 2.3: The increase in viscosity $\frac{\mu_s}{\mu_0}$ as a function of concentration ϕ.

The concentration is represented by the x-axis and the increase in viscosity by the y-axis. A curve can be seen, as the concentration increases, so does the viscosity. When the concentration increases, there is less space as there are more particles. The particles experience interaction with not only the fluid but also with other particles. As a consequence, the settling speed of particles decreases. This phenomenon is called hindered settling.

2.2 Experimental plan

In this section the experimental set-up will be presented, as well as the experimental procudure that was followed before, during and after the experiments. And at last an overview is presented of the experiments performed for this thesis.

2.2.1 Experimental set-up

In this subsection the experimental set-up is presented. All equipment used during the experiments are listed in table 2.1. The main equipment used for the experiments are listed below with specifications and/or elaboration of the use:

- A transparant perspex tank was used to perform the experiments in with measurements L x W x H = 300 x 20 x 40 cm. The channel is used previously for the study of [Stovers, 2016]. See figure 2.4.
- Led panels were placed behind the channel for a better visualisation of the gravity current.
- A SONY A7 mark III camera with a 24mm SONY camera lens was used to record the experiment. All footage was recorded with a 1080p video setting. By analysing the footage, the front nose position of the current could be determined in time making it possible to derive the velocity. Furthermore, the recordings also made it possible to see if there were any unexpected or odd events during the experiment.
- The vacuum cleaner that was used to collect samples with was a Karcher vacuum cleaner. This method was chosen as a common method used in literature to establish the deposit particle/density distribution in the sediment is vacuuming using tube at specific intervals in the tank. Both [Bonnecaze et al., 1993] and [Hallworth and Huppert, 1998] made use of this technique and have proven it to be a successful method. Samples are taken and the particle size distribution and weight is determined using a scale with 0.1g precision. The Kärcher vacuum cleaner operates in an identical way.
- The mixing is performed using a perforated mixing tool which is moved vertically through the heavy fluid to keep the particles suspended. This method causes only small turbulences, in the form of vortices that occur when water is forced through the gaps in the plate, that have very little impact on the current once the barrier is removed.
- Waterproof sandpaper with p60, which is equivalent to a granule size of 180 µm.
- Geba Weis sand with d_{50} = 103 µm claimed but 138 µm measured, was used in the suspension. The sieve curve in Appendix A shows a more detailed presentation of the d_{50}.

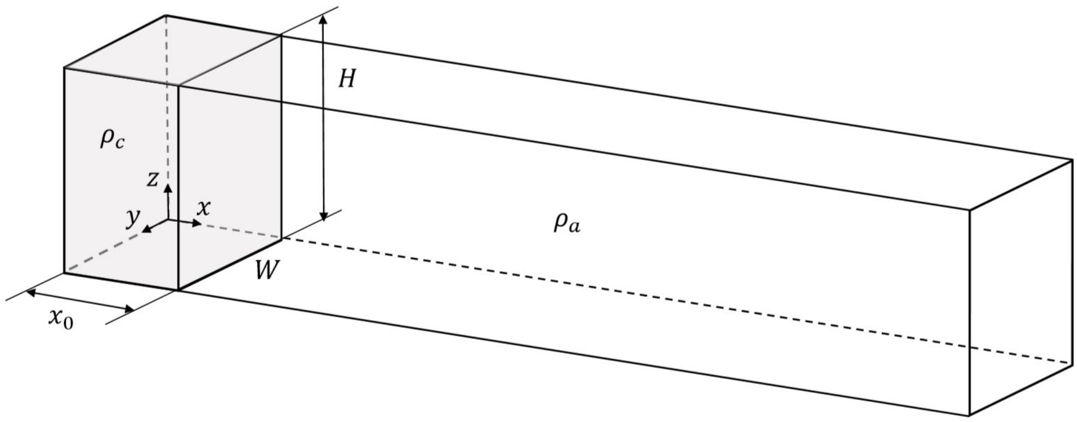

Figure 2.4: Perspex tank with a lock gate.

Table 2.1: Equipment for lock-exchange experiment.

#	Lock-exchange
1.	Perspex tank with a lock gate (L = 300 cm, W = 20 cm, H = 40 cm)
2.	LED panels
3.	Camera (Sony A7iii - 120 fps)
4.	Thermometer
5.	Karcher vacuum cleaner
6.	Perforated mixing tool
7.	Waterproof sandpaper P60
8.	Geba weis sand (D50 = 103 μm, 138 μm measured)
9.	Scale with 0.1 g precision
10.	PSD sieves 63 μm - 250 μm
11.	Oven

2.2.2 Experimental procedure

Before the experiments can be performed, certain preparations have to be made. Firstly, the sand is washed. The purpose of washing the sand is to remove the unnecessary fine particles that could make the suspension cloudy. This has to be avoided as this would make it difficult to analyse the behaviour of the current (on film). After the washing, the sand has to be dried completely. To speed up this process, the sand is put in an oven until dry. When the sand is completely dry, it is weighed carefully.

After washing, drying and weighing the sand, it is ready to be used to make a homogeneous suspension in the lock-gate part of the tank. It is vital that the mixing that has to take place in order to create the suspension, is done carefully to minimise disturbance and flows that could have effects on the gravity current. When this is achieved, the lock-gate can be removed. When the heavier fluid is released, a gravity current will travel through the channel. This current should not reflect against the back wall as this will influence the results. Once the current disappears and all the sediment has settled, samples are taken at predetermined places on the bottom of the channel using the vacuum cleaner.

Finally, the taken samples can be analysed. The particle size distribution (sieve analysis) is and weight are established after drying. The evolution of the gravity current can be analysed using the video material and the velocity can be derived.

2.2.3 Overview of experiments

A total of 111 lock release gravity current experiments were performed. The parameters of each experiment are listed in the tables. The experiments can be divided in 3 different types which were carried in threefold. Carrying out each experiment multiple times led to greater sample sizes so more sand was available for the sieve analysis, as a minimum amount is necessary to determine the particle size distribution at specific intervals over the run out length of the gravity current. This also made it possible to assess the consistency of the experiments, which turned out positively.

Experiments part 1

The first 30 experiments were performed using a mono-disperse suspension, see table 2.2. For the experiments 31 to 51, a bi-disperse mixture was used, see table 2.3.

Table 2.2: Experiments part 1: Mono-disperse mixture

#	Sample	Dimensions			Sand			Parameters				
		w_0 [m]	H [m]	x_0 [m]	Type	Diameter [μm]	Mass [g]	ϕ -	ρ_c [kg/m3]	g' [m/s2]	T [°C]	γ -
1	1	0,2	0,15	0,2	Geba	90-125	3248	0,2	1329	3,24	14,3	0,75
2	1	0,2	0,15	0,2	Geba	90-125	3248	0,2	1329	3,24	14,1	0,75
3	1	0,2	0,15	0,2	Geba	90-125	3248	0,2	1329	3,24	14,4	0,75
4	2	0,2	0,15	0,2	Geba	150-180	3248	0,2	1329	3,24	14,8	0,75
5	2	0,2	0,15	0,2	Geba	150-180	3248	0,2	1329	3,24	15,1	0,75
6	2	0,2	0,15	0,2	Geba	150-180	3248	0,2	1329	3,24	14,9	0,75
7	3	0,2	0,12	0,2	Geba	90-125	3897,5	0,3	1495	4,86	14,4	0,67
8	3	0,2	0,12	0,2	Geba	90-125	3897,5	0,3	1495	4,86	14,2	0,67
9	3	0,2	0,12	0,2	Geba	90-125	3897,5	0,3	1495	4,86	14,2	0,67
10	4	0,2	0,12	0,2	Geba	150-180	3897,5	0,3	1495	4,86	15,4	0,67
11	4	0,2	0,12	0,2	Geba	150-180	3897,5	0,3	1495	4,86	15,7	0,67
12	4	0,2	0,12	0,2	Geba	150-180	3897,5	0,3	1495	4,86	15,8	0,67
13	5	0,2	0,12	0,2	Geba	90-125	4546,5	0,35	1577	5,66	14,2	0,63
14	5	0,2	0,12	0,2	Geba	90-125	4546,5	0,35	1577	5,66	14,6	0,63
15	5	0,2	0,12	0,2	Geba	90-125	4546,5	0,35	1577	5,66	14,5	0,63
16	6	0,2	0,12	0,2	Geba	150-180	4546,5	0,35	1577	5,66	13,9	0,63
17	6	0,2	0,12	0,2	Geba	150-180	4546,5	0,35	1577	5,66	14	0,63
18	6	0,2	0,12	0,2	Geba	150-180	4546,5	0,35	1577	5,66	14,3	0,63
19	7	0,2	0,12	0,2	Geba	90-125	5196,5	0,4	1660	6,47	15,1	0,6
20	7	0,2	0,12	0,2	Geba	90-125	5196,5	0,4	1660	6,47	15,4	0,6
21	7	0,2	0,12	0,2	Geba	90-125	5196,5	0,4	1660	6,47	15,3	0,6
22	8	0,2	0,12	0,2	Geba	150-180	5196,5	0,4	1660	6,47	16,5	0,6
23	8	0,2	0,12	0,2	Geba	150-180	5196,5	0,4	1660	6,47	16,4	0,6
24	8	0,2	0,12	0,2	Geba	150-180	5196,5	0,4	1660	6,47	16,5	0,6
25	9	0,2	0,12	0,2	Geba	90-125	3248	0,25	1412,5	4,05	14,8	0,71
26	9	0,2	0,12	0,2	Geba	90-125	3248	0,25	1412,5	4,05	14,8	0,71
27	9	0,2	0,12	0,2	Geba	90-125	3248	0,25	1412,5	4,05	14,9	0,71
28	10	0,2	0,12	0,2	Geba	150-180	3248	0,25	1412,5	4,05	15,6	0,71
29	10	0,2	0,12	0,2	Geba	150-180	3248	0,25	1412,5	4,05	15,3	0,71
30	10	0,2	0,12	0,2	Geba	150-180	3248	0,25	1412,5	4,05	15,3	0,71

Table 2.3: Experiments part 1b: Bi-disperse mixture

#	Sample	Dimensions			Sand		Parameters					
		w_0 [m]	H [m]	x_0 [m]	Type	d_{50} [μm]	Mass [g]	ϕ -	ρ_c [kg/m3]	g' [m/s2]	T [°C]	γ -
31	11	0,2	0,2	0,2	Geba	bi-mix	2165,5	0,1	1165	1,62	15,8	0,86
32	11	0,2	0,2	0,2	Geba	bi-mix	2165,5	0,1	1165	1,62	16,1	0,86
33	11	0,2	0,2	0,2	Geba	bi-mix	2165,5	0,1	1165	1,62	16,3	0,86
34	12	0,2	0,15	0,2	Geba	bi-mix	2436	0,15	1247,5	2,43	16,2	0,8
35	12	0,2	0,15	0,2	Geba	bi-mix	2436	0,15	1247,5	2,43	16,5	0,8
36	12	0,2	0,15	0,2	Geba	bi-mix	2436	0,15	1247,5	2,43	16,4	0,8
37	13	0,2	0,15	0,2	Geba	bi-mix	3248	0,2	1329,8	3,24	15,4	0,75
38	13	0,2	0,15	0,2	Geba	bi-mix	3248	0,2	1329,8	3,24	15,6	0,75
39	13	0,2	0,15	0,2	Geba	bi-mix	3248	0,2	1329,8	3,24	15,5	0,75
40	14	0,2	0,12	0,2	Geba	bi-mix	3248	0,25	1412,5	4,05	16,2	0,71
41	14	0,2	0,12	0,2	Geba	bi-mix	3248	0,25	1412,5	4,05	16,4	0,71
42	14	0,2	0,12	0,2	Geba	bi-mix	3248	0,25	1412,5	4,05	16,5	0,71
43	15	0,2	0,12	0,2	Geba	bi-mix	3897,5	0,3	1495	4,86	15,7	0,67
44	15	0,2	0,12	0,2	Geba	bi-mix	3897,5	0,3	1495	4,86	15,3	0,67
45	15	0,2	0,12	0,2	Geba	bi-mix	3897,5	0,3	1495	4,86	15,6	0,67
46	16	0,2	0,12	0,2	Geba	bi-mix	4546,5	0,35	1577	5,66	16,2	0,63
47	16	0,2	0,12	0,2	Geba	bi-mix	4546,5	0,35	1577	5,66	16,6	0,63
48	16	0,2	0,12	0,2	Geba	bi-mix	4546,5	0,35	1577	5,66	16,3	0,63
49	17	0,2	0,12	0,2	Geba	bi-mix	5196,5	0,4	1660	6,47	15,9	0,6
50	17	0,2	0,12	0,2	Geba	bi-mix	5196,5	0,4	1660	6,47	16,2	0,6
51	17	0,2	0,12	0,2	Geba	bi-mix	5196,5	0,4	1660	6,47	16,5	0,6

Experiments part 2

The second group of experiments were performed with a poly-disperse suspension on either a rough bed or a smooth bed. Tests 52 to 72 were run on a rough bed which was created by adding waterproof sandpaper to the bottom, see table 2.4. Experiments 73 to 93 were performed on a smooth bed, see table 2.5.

Table 2.4: Experiments part 2a: Poly-disperse mixture with rough bed

#	Sample	Dimensions			Sand			Parameters				
		w_0 [m]	H [m]	x_0 [m]	Type	d_{50} [μm]	Mass [g]	ϕ -	ρ_c [kg/m3]	g' [m/s2]	T [°C]	γ -
52	18	0,2	0,2	0,2	Geba	138	2165,5	0,1	1165	1,62	10,4	0,86
53	18	0,2	0,2	0,2	Geba	138	2165,5	0,1	1165	1,62	10,7	0,86
54	18	0,2	0,2	0,2	Geba	138	2165,5	0,1	1165	1,62	10,2	0,86
55	19	0,2	0,15	0,2	Geba	138	2436	0,15	1247,5	2,43	10,9	0,8
56	19	0,2	0,15	0,2	Geba	138	2436	0,15	1247,5	2,43	11,2	0,8
57	19	0,2	0,15	0,2	Geba	138	2436	0,15	1247,5	2,43	11,2	0,8
58	20	0,2	0,15	0,2	Geba	138	3248	0,2	1329,8	3,24	10,1	0,75
59	20	0,2	0,15	0,2	Geba	138	3248	0,2	1329,8	3,24	10,3	0,75
60	20	0,2	0,15	0,2	Geba	138	3248	0,2	1329,8	3,24	10,1	0,75
61	21	0,2	0,12	0,2	Geba	138	3248	0,25	1412,5	4,05	11,4	0,71
62	21	0,2	0,12	0,2	Geba	138	3248	0,25	1412,5	4,05	11,3	0,71
63	21	0,2	0,12	0,2	Geba	138	3248	0,25	1412,5	4,05	11,4	0,71
64	22	0,2	0,12	0,2	Geba	138	3897,5	0,3	1495	4,86	11,7	0,67
65	22	0,2	0,12	0,2	Geba	138	3897,5	0,3	1495	4,86	11,5	0,67
66	22	0,2	0,12	0,2	Geba	138	3897,5	0,3	1495	4,86	11,7	0,67
67	23	0,2	0,12	0,2	Geba	138	4546,5	0,35	1577	5,66	10,8	0,63
68	23	0,2	0,12	0,2	Geba	138	4546,5	0,35	1577	5,66	10,5	0,63
69	23	0,2	0,12	0,2	Geba	138	4546,5	0,35	1577	5,66	10,6	0,63
70	24	0,2	0,12	0,2	Geba	138	5196,5	0,4	1660	6,47	10,9	0,6
71	24	0,2	0,12	0,2	Geba	138	5196,5	0,4	1660	6,47	11,2	0,6
72	24	0,2	0,12	0,2	Geba	138	5196,5	0,4	1660	6,47	11,3	0,6

Table 2.5: Experiments part 2b: Poly-disperse mixture with smooth bed

#	Sample	Dimensions			Sand			Parameters				
		w_0 [m]	H [m]	x_0 [m]	Type	d_{50} [μm]	Mass [g]	ϕ -	ρ_c [kg/m3]	g' [m/s2]	T [°C]	γ -
73	25	0,2	0,2	0,2	Geba	138	2165,5	0,1	1165	1,62	12,8	0,86
74	25	0,2	0,2	0,2	Geba	138	2165,5	0,1	1165	1,62	12,4	0,86
75	25	0,2	0,2	0,2	Geba	138	2165,5	0,1	1165	1,62	12,7	0,86
76	26	0,2	0,15	0,2	Geba	138	2436	0,15	1247,5	2,43	12,4	0,8
77	26	0,2	0,15	0,2	Geba	138	2436	0,15	1247,5	2,43	12,6	0,8
78	26	0,2	0,15	0,2	Geba	138	2436	0,15	1247,5	2,43	12,9	0,8
79	27	0,2	0,15	0,2	Geba	138	3248	0,2	1329,8	3,24	11,9	0,75
80	27	0,2	0,15	0,2	Geba	138	3248	0,2	1329,8	3,24	12,2	0,75
81	27	0,2	0,15	0,2	Geba	138	3248	0,2	1329,8	3,24	12,5	0,75
82	28	0,2	0,12	0,2	Geba	138	3248	0,25	1412,5	4,05	10,8	0,71
83	28	0,2	0,12	0,2	Geba	138	3248	0,25	1412,5	4,05	11,2	0,71
84	28	0,2	0,12	0,2	Geba	138	3248	0,25	1412,5	4,05	11,3	0,71
85	29	0,2	0,12	0,2	Geba	138	3897,5	0,3	1495	4,86	10,4	0,67
86	29	0,2	0,12	0,2	Geba	138	3897,5	0,3	1495	4,86	10,5	0,67
87	29	0,2	0,12	0,2	Geba	138	3897,5	0,3	1495	4,86	10,4	0,67
88	30	0,2	0,12	0,2	Geba	138	4546,5	0,35	1577	5,66	10,7	0,63
89	30	0,2	0,12	0,2	Geba	138	4546,5	0,35	1577	5,66	10,9	0,63
90	30	0,2	0,12	0,2	Geba	138	4546,5	0,35	1577	5,66	10,7	0,63
91	31	0,2	0,12	0,2	Geba	138	5196,5	0,4	1660	6,47	11,3	0,6
92	31	0,2	0,12	0,2	Geba	138	5196,5	0,4	1660	6,47	11,7	0,6
93	31	0,2	0,12	0,2	Geba	138	5196,5	0,4	1660	6,47	11,4	0,6

Experiments part 3

Finally, in the third group of experiments, the influence of temperature was measured. Tests 94 to 111 were performed using water with a higher temperature. These tests were compared to the tests 73 to 93 in the second group performed on a smooth bottom surface.

Table 2.6: Experiments part 3: Poly-disperse mixture with a higher temperature

#	Sample	Dimensions			Sand			Parameters				
		w_0 [m]	H [m]	x_0 [m]	Type	d_{50} [μm]	Mass [g]	ϕ -	ρ_c [kg/m3]	g' [m/s2]	T [°C]	γ -
94	32	0,2	0,2	0,2	Geba	138	2165,5	0,1	1165	1,62	21,8	0,86
95	32	0,2	0,2	0,2	Geba	138	2165,5	0,1	1165	1,62	21,7	0,86
96	32	0,2	0,2	0,2	Geba	138	2165,5	0,1	1165	1,62	21,3	0,86
97	33	0,2	0,15	0,2	Geba	138	2436	0,15	1247,5	2,43	21,2	0,8
98	33	0,2	0,15	0,2	Geba	138	2436	0,15	1247,5	2,43	21,5	0,8
99	33	0,2	0,15	0,2	Geba	138	2436	0,15	1247,5	2,43	21,4	0,8
100	34	0,2	0,12	0,2	Geba	138	3248	0,25	1412,5	4,05	21,9	0,71
101	34	0,2	0,12	0,2	Geba	138	3248	0,25	1412,5	4,05	21,7	0,71
102	34	0,2	0,12	0,2	Geba	138	3248	0,25	1412,5	4,05	22	0,71
103	35	0,2	0,12	0,2	Geba	138	3897,5	0,3	1495	4,86	21,2	0,67
104	35	0,2	0,12	0,2	Geba	138	3897,5	0,3	1495	4,86	21,4	0,67
105	35	0,2	0,12	0,2	Geba	138	3897,5	0,3	1495	4,86	21,5	0,67
106	36	0,2	0,12	0,2	Geba	138	4546,5	0,35	1577	5,66	22,6	0,63
107	36	0,2	0,12	0,2	Geba	138	4546,5	0,35	1577	5,66	22,3	0,63
108	36	0,2	0,12	0,2	Geba	138	4546,5	0,35	1577	5,66	22,7	0,63
109	37	0,2	0,12	0,2	Geba	138	5196,5	0,4	1660	6,47	22,1	0,6
110	37	0,2	0,12	0,2	Geba	138	5196,5	0,4	1660	6,47	21,7	0,6
111	37	0,2	0,12	0,2	Geba	138	5196,5	0,4	1660	6,47	21,8	0,6

2.3 Discussion experiments

During the experiments, four difficulties were encountered and tried to be mitigated, in order to perform the experiments as well as possible. In this section these four difficulties and their mitigations are discussed and presented.

2.3.1 Reaching the end-wall

When the gravity current reaches the end-wall of the channel, it will cause it to reflect back. If this occurs during the experiment, the analysis of particle-size distribution cannot be performed as the current will travel back and deposit particles doing so. This could be avoided by adding an additional part at the end of the tank that would be wider than the channel itself. By doing so, the current can spread axially which will reduce the chances of reflection. Another possible way of avoiding this problem could be to reduce the velocities of the current which leads to a shorter run-out length. This could be established by reducing the initial height of the current as this will lead to a reduction in potential energy in the system.

2.3.2 Mixing

An important part of the experiment is creating a homogeneous suspension. The particles in the heavier fluid behind the barrier will start to settle over time if the fluid is stationary. To avoid this, the fluid has to be mixed in order for the particles to stay suspended. However, before the experiment can be executed, the fluid has to be stationary and mixing can cause disturbances such as turbulence or flows. Therefore, the mixing has to be carried out in such a way that it causes minimal disturbances. For this reason, the mixing is performed using a perforated plate which is moved vertically through the heavy fluid to keep the particles suspended. This method causes only small turbulences, in the form of vortices that occur when water is forced through the gaps in the plate, that have very little impact on the current once the barrier is removed.

2.3.3 Turbulence

The significance of initial turbulence behind the lock gate has been investigated by [Necker et al., 2005]. They compared three cases with different initial kinetic energy levels and found that initial turbulence enhances mixing within the current (fluid) strongly. However, the influence of the amount of initial turbulence on the behaviour of the gravity current seems to be weak as it is dissipated both by sedimentation and by the conversion of the initially available potential energy into convective motion(macroscopic flow) early in the current development.

2.3.4 Parallax effect (error)

When an object appears as if it is positioned differently when it is viewed from different angles or positions, it is called a parallax error. In the experiment, this can occur when the actual view covered by the camera lens is different than the view seen through the viewfinder. The effect especially becomes evident when moving objects are filmed close to the camera. This makes observation difficult as the gravity current travels while the camera is fixed. In order to decrease the chances of a parallax error, the camera can be placed at a greater distance from the tank and the spatial increments can be placed on the front side of the tank.

Chapter 3

Results Experiments

Several experiments were carried out in order to answer each of the main questions formulated in this thesis. In this section, each question will be linked to a specific experiment.

- The first question was:

  What is the influence of particle size(s) of the mixture for the behaviour of a gravity current?

  Each particle in a poly-disperse suspension has a different settling velocity. For this reason, the experiments are focused on analyzing the behaviour of different particle sizes and its influence on the gravity current. Experiments 1 to 30 were carried out using a mono-disperse mixture with 90 μm and 150 μm particles, respectively. These particle sizes have a settling ratio of around 2:5. The experiments with a mono-disperse mixture are referred to as: 'mono-experiments' in this thesis.

  In addition, experiments 31 to 51 were carried out with a mixture consisting of 90- as well as 150 μm particles in a 50/50 ratio. These experiments are also referred to as: 'bi-disperse/mixed experiments' in this thesis.

  The influence of the particle sizes on the 4 phases of the gravity current were analysed in each of the 3 experiments. These are presented in section 3.1.1. Additionally, the run-out length was determined and these are presented in section 3.1.2. Finally, the influence of the particles sizes on the PSD and the deposit density of the gravity current was analysed and presented in section 3.1.3.

- The second question that was formulated was:

  What is the influence of bed roughness on the behaviour of a gravity current?

  In order to research the influence of the underground on the gravity current, experiments were carried out using either a smooth bed or a rough bed. To make the rough bed, waterproof sandpaper was attached to the bottom. Waterproof sandpaper with p60, which is equivalent to a granule size of 180 μm was used. This setup was used to be able to carry out the experiments over a rough bed in a similar way to the experiments over a smooth bed. The suspension used in these experiments is a poly-disperse mixture consisting of Geba Weis sand with D50 of 138 μm. These experiments are also referred to as 'rough bed experiments' and 'smooth bed experiments'.

  To properly answer the second question, the influence of bed roughness on the 4 phases was determined. These are presented in section 3.2.1. Furthermore, the influence on the run-out length is presented in section 3.2.2. Lastly, the influence of the bed roughness on the PSD was observed in section 3.2.3.

- The final question was:

  What is the influence of temperature of the mixture for the behaviour of a gravity current?

  To answer this question, experiments focused on temperature were conducted. A set of experiments was carried out, see table 2.6 for an overview. The methods used in these experiments are similar to the previous lock-exchange experiments. All parameters were unaltered except for the temperature of the suspension. Numbers 73 to number 93 were experiments using a suspension that was 11 degrees Celsius, also referred to as: 'cold water experiments'. In experiments 94 to 111, the suspension was around 22 degrees Celsius, also referred to as 'warm water experiments'. The suspension used in these experiments is a poly-disperse mixture consisting of Geba Weis sand with D50 of 138μm.

  Similarly to the previously discussed experiments, the 4 phases were analysed and are displayed in section 3.3.1. The run-out length is shown in section 3.3.2 and finally the influence on the PSD was researched as well in section 3.3.3.

For a good understanding of what the figures in this chapter present, a summary is given below:

- 4 phases: The horizontal axis displays the dimensionless distance $^{l}/_{H}$. On the vertical axis we find the dimensionless velocity represented by the Froude number $Fr = ^{u}/_{\sqrt{g'}H}$, where u is the velocity at the nose of the current, g' is the reduced gravity and H is the initial height.

- Run out length: The horizontal axis displays the concentration of the mixture and on the vertical axis we find the dimensionless distance $^{l}/_{H}$.

- PSD: Carrying out each experiment in threefold led to greater sample sizes so more sand was available for the sieve analysis, as a minimum amount is necessary to determine the particle size distribution at specific intervals over the run out length of the gravity current. The specific intervals are at every 30 cm and a sample was taken at each interval. These values were converted to dimensionless distance values. The dimensionless distance values that correspond with the specific sample points are displayed on the left side of each figure. The values can be seen in the box and are linked to the different colours.

3.1 Mono-Mix experiments

3.1.1 4 Phases

The 4 different concentrations are portrayed in the upper part of figure 3.1 in which the 4 phases can be observed. Phase 1 is clearly identifiable, this applies to all concentrations displayed. After phase 1, few differences can be seen between the mixtures at different concentrations. Remarkably when phase 3 sets in, considerable differences are observed. Phase 3 sets in earlier in the current consisting of larger particles than in the current consisting of smaller particles or a mixture of both.

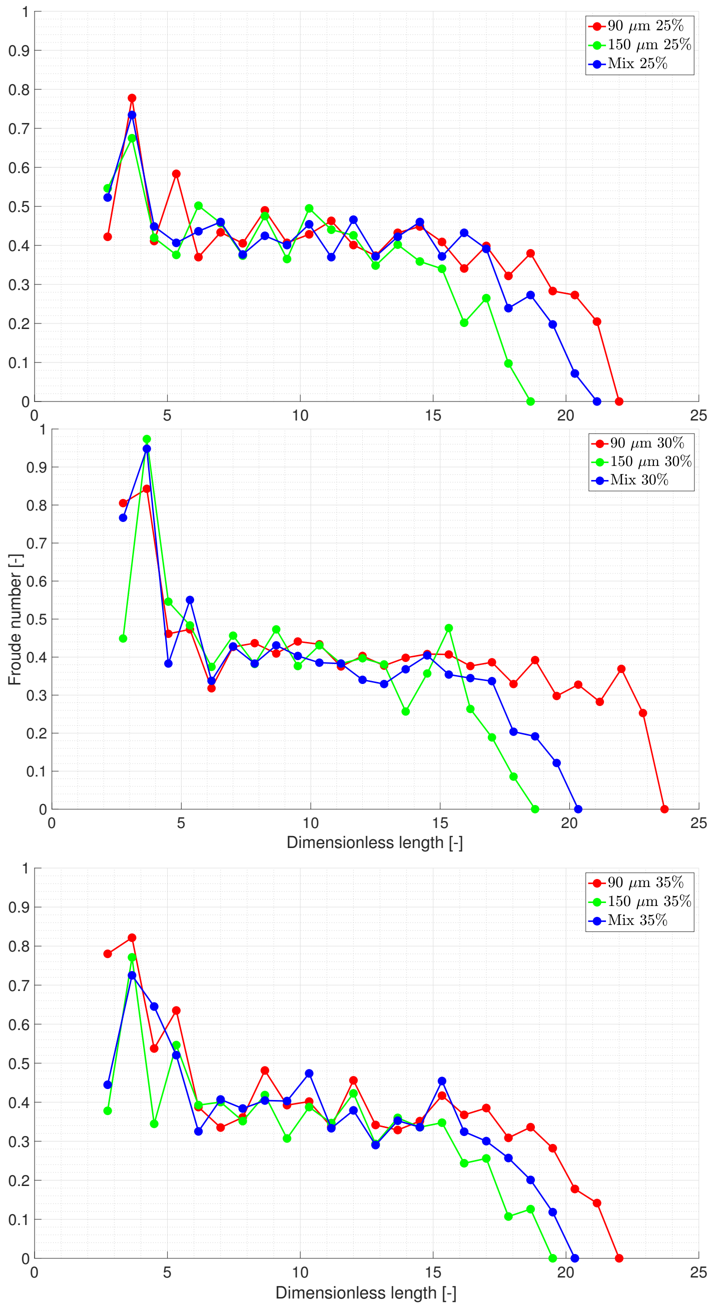

Figure 3.1: Four phases of the mono-disperse and bi-disperse mixtures.

3.1.2 Run-out length

In figure 3.2 it can be observed that the current consisting of 90 μm particles has a longer run-out length at all concentrations. The current consisting of 150 micron meter has a shorter run-out length at all concentrations. Additionally, the mix current seems to lean towards the behaviour regarding the run-out length of the 90 μm particle current at concentrations up to 30%. When the concentration is increased above 30%, the run-out length of the mix current becomes more similar to that of the 150 μm particle current. This is also presented in figure 3.3, where the particle size domination is shown for all of the bi-disperse experiments.

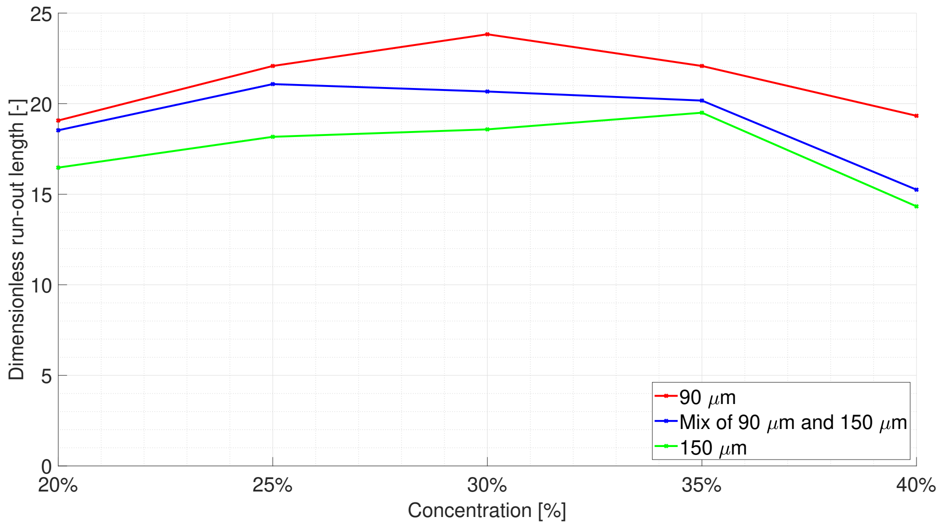

Figure 3.2: Run-out length of measurements.

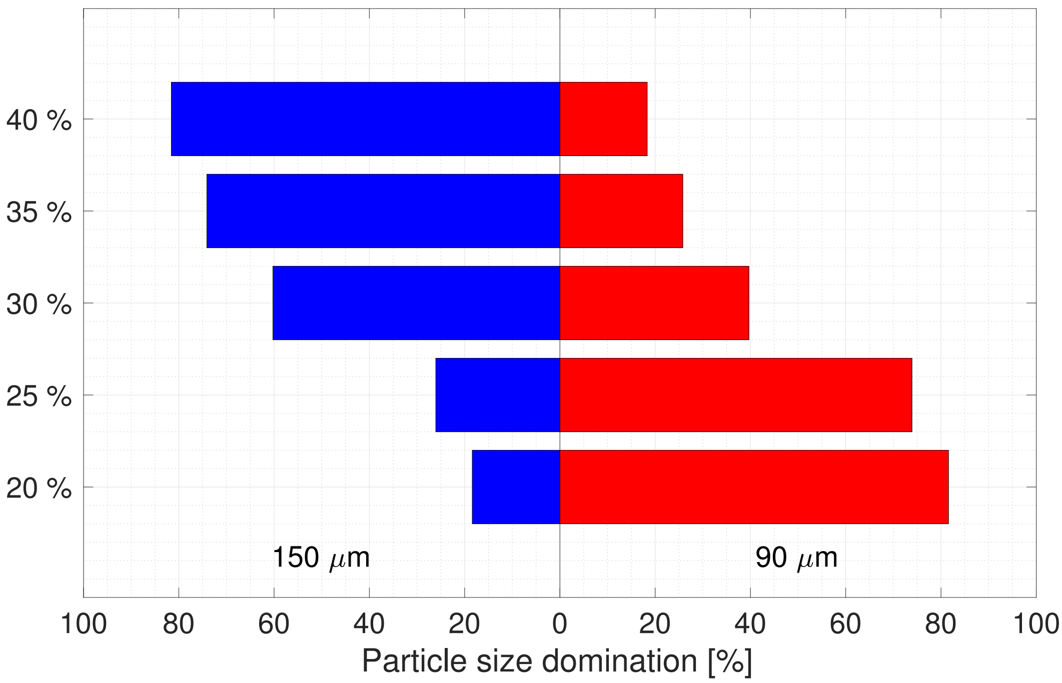

Figure 3.3: Influence of particle sizes (90μ m and 150μ m) on the run-out length of the bi-disperse mixture.

3.1.3 Influence of particle concentration

The influence of the particle concentration on mono- and bi-disperse mixtures and their differences are discussed in the following section.

Mono-disperse mixture

The deposition density at different concentrations of the two mono-disperse mixtures (90 μm and 150 μm) are shown in figure 3.4. It is clearly noticeable that the 150 μm mono-dispersed mixture has a higher deposition density at all concentrations until the dimensionless length of 10m (is reached) with a concentration of 40%. Beyond this point, a shift occurs at a concentration of 40% which also occurs at the other concentrations but further to the right along the x-axis. Now, smaller particles make up a larger portion of the deposition density the larger particles in contrast to the beginning. This is expected as larger particles settle faster and thus lead to a higher deposition density in the beginning. The shift occurs when most of these larger particles have settled. There are simply more smaller particles left beyond this point which explains why later on the deposition density contains more smaller particles.

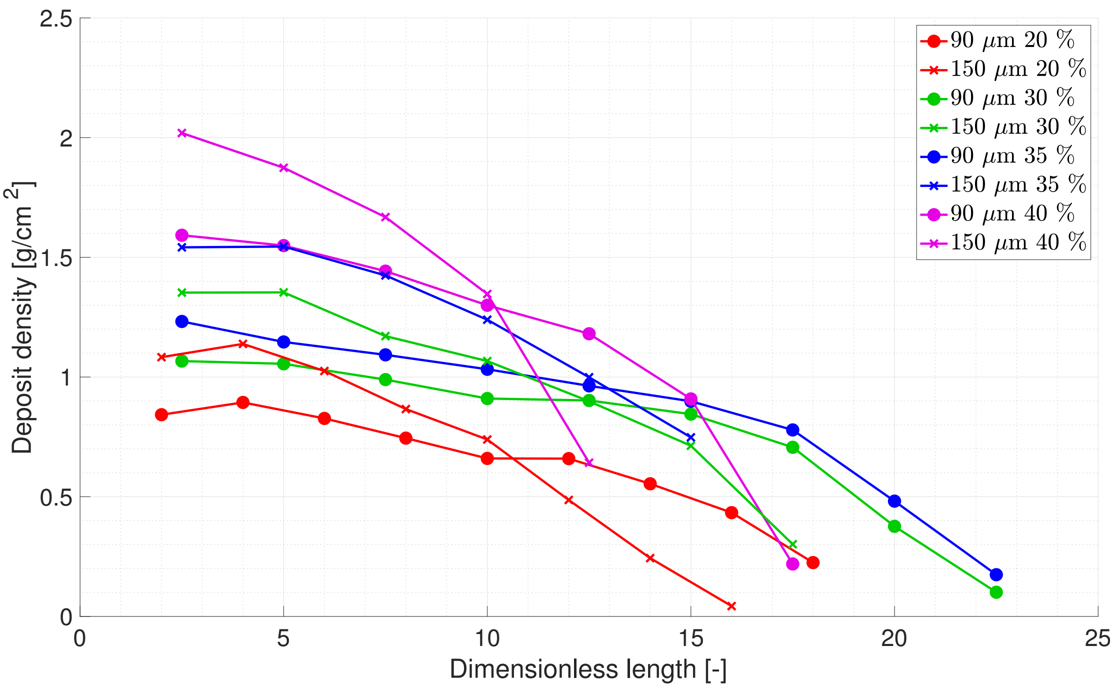

Figure 3.4: Deposition density of the Mono-disperse mixtures.

Bi-disperse mixture

The ratio between the smaller and bigger particles at different concentrations is displayed in figure 3.5. As can be seen from this figure, the ratio changes at lower concentrations. At low concentrations, the ratio of smaller particles is greater than of larger particles which can be seen as a steep slope in the figure. As the concentration increases, the ratio of larger particles increases. Starting at a 30% concentration and up, the slope becomes more horizontal until the ratio becomes nearly equal for both particle sizes.

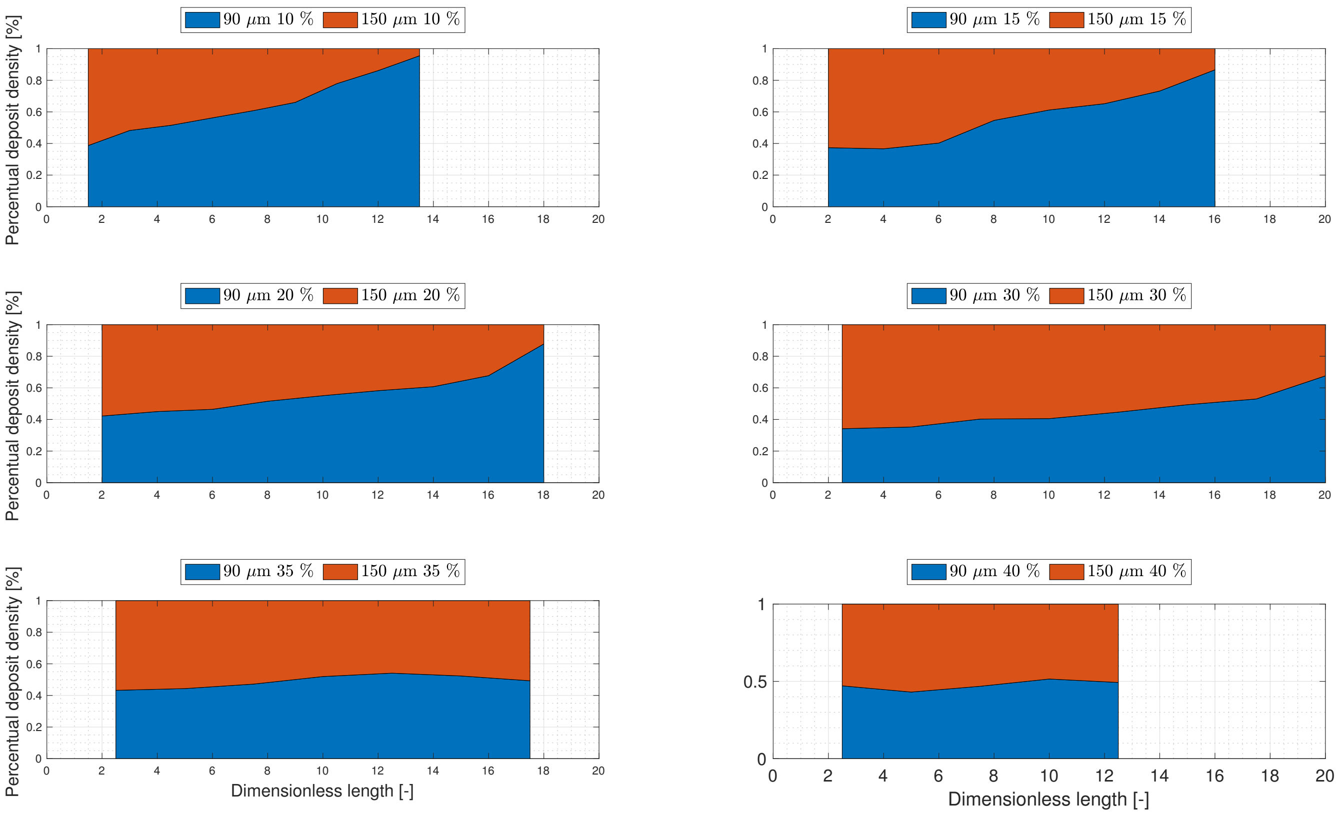

Figure 3.5: Deposition density of the bi-disperse mixtures.

In figure 3.6, the deposition density of the bi-disperse mixture is shown. Specifically, the contribution of each particle size to the deposition density is studied. Subsequently, the differences between the the deposition density of the mono- and bi-disperse mixtures are also observed.

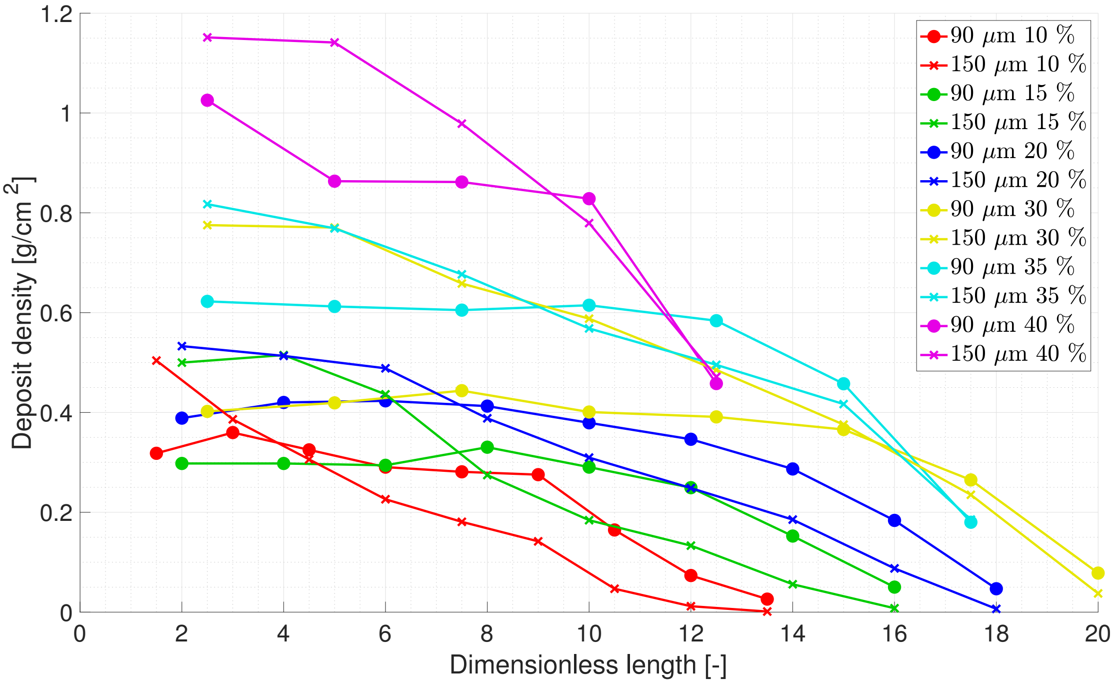

Figure 3.6: Deposit density of the bi-disperse mixtures.

The differences between the mono- and bi-dispersed mixtures are displayed in figure 3.7. There is little difference at lower concentrations as can be seen in the figure. At a concentration of 30%, the ratio of the 90 μm particles in the deposition density is higher in the mono-dispersed mixture. For the 150μm-sized particles, the opposite is true. At 35% the deposition density is comparable between the two suspensions. However, the 90 μm particles in the bi-dispersed mixture settle earlier compared to the graphs before creating a relatively big difference at the end. At 40%, the deposition density of both particles in the mixed suspension is greater than in the mono-dispersed suspension.

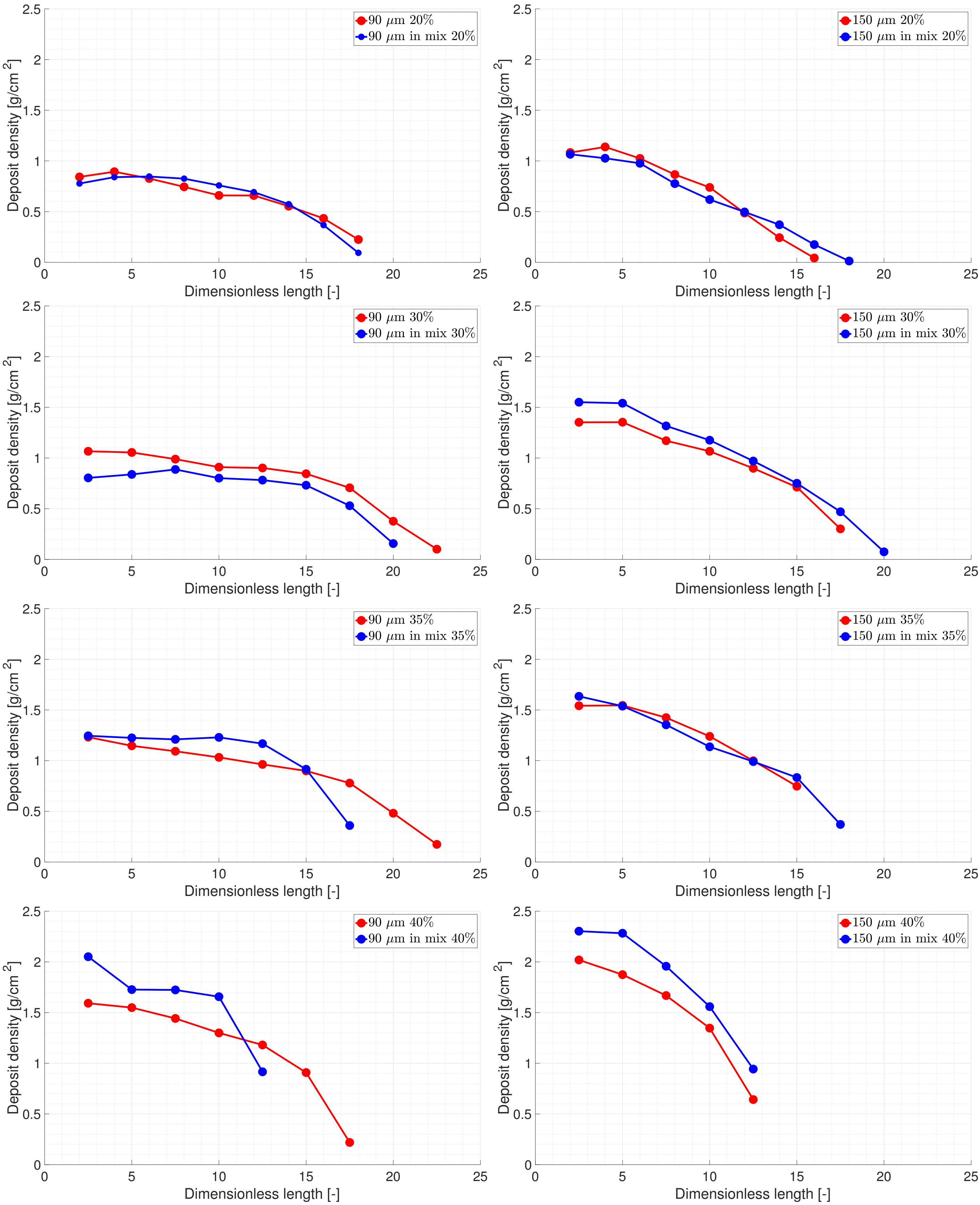

Figure 3.7: Deposit density of the mono-disperse and bi-disperse mixtures.

3.2 Bed roughness

3.2.1 4 Phases

In figure 3.8 the four phases of the experiments with a smooth and a rough bed can be seen. The experiments were performed at different concentrations, starting at 15%. Again, the concentration was increased by 5% up to 40%. A total of 6 different concentrations were used.
The four phases can easily be distinguished in the smooth bed (experiments) at all concentrations. For the rough bed experiments, that doesn't seem to apply. Something unusual seems to happen during the experiments with a rough bed, as can be seen in the figure. The first phase seems to be absent at lower concentrations (15 / 20%). This has not be seen during other experiments. What appears to be happening is that the gravity current goes straight to the constant phase, also called the second phase. At a concentration of 25% , phase one starts to become slightly more visible but is followed by a bumpy constant phase in contrast to the normally smooth constant phase. From a concentration of 30% and higher, the gravity current proceeds as normal. A clear first phase can be distinguished that is followed by a nearly constant second phase, a third and a fourth phase.
Additionally, the figures show that the third phase sets in earlier in all rough bed experiments except for the 15% experiment result that shows a negligibly small difference.

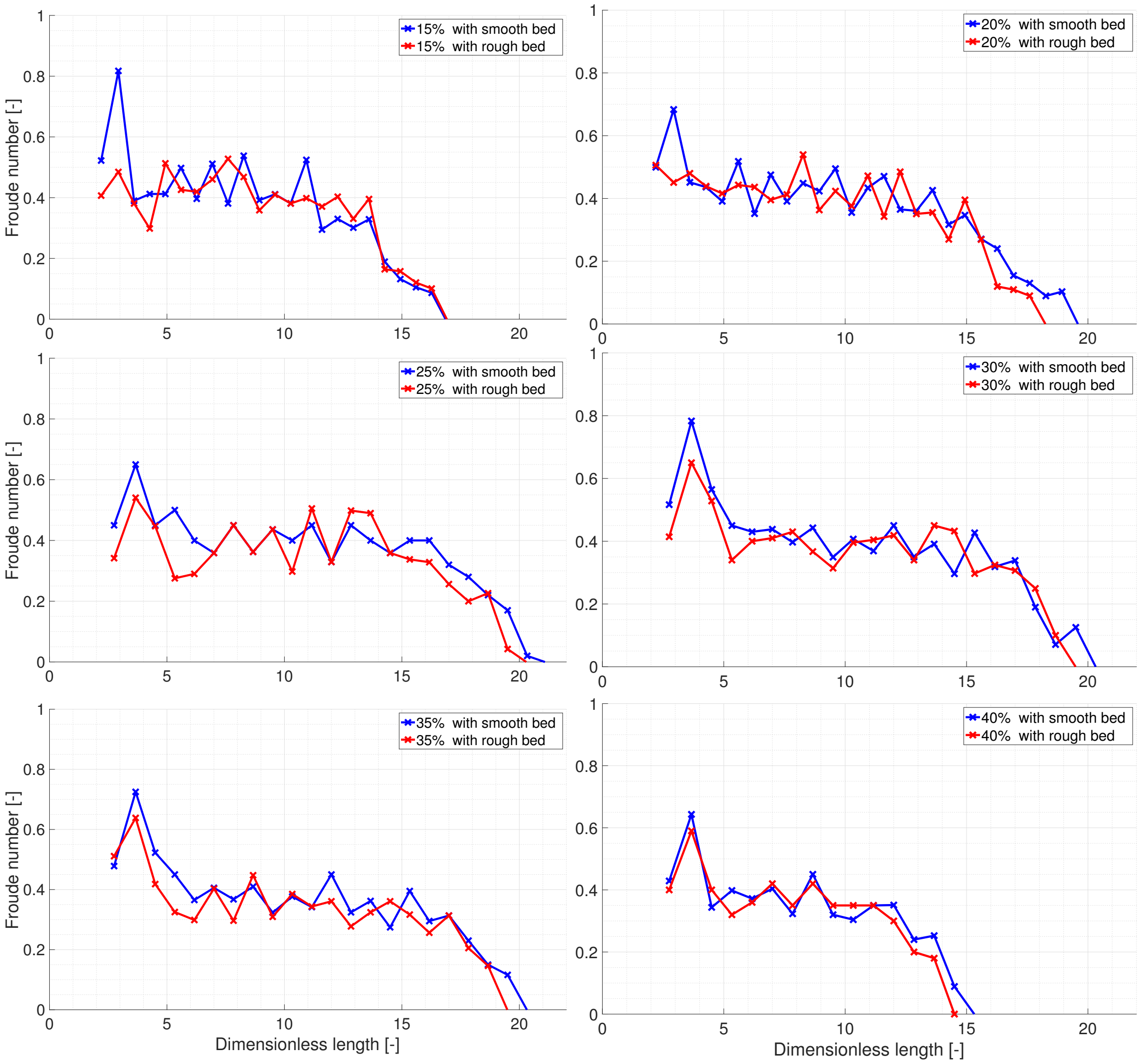

Figure 3.8: Four phases of a smooth and rough bed.

3.2.2 Run-out length

In table 3.1, the results of the experiments performed on a smooth and a rough bed are displayed and can easily be compared. A clear difference can be seen between the two, the run-out length is shorter for all experiments over a rough bed compared to the smooth bed experiments.

Table 3.1: Run-out length of smooth and rough bed.

	Smooth bed	Rough bed
10%	13,45	13,20
15%	17,20	16,87
20%	18,80	18,20
25%	21,17	20,25
30%	22,08	19,50
35%	21,09	19,50
40%	17,06	14,33

3.2.3 Particle size distribution

The results of the experiments performed on a rough and smooth bed are shown in figures 3.9, 3.10 and 3.11. The smooth bed experiments can be seen on the left side and the rough bed experience on the right. The figures show that the PSD becomes denser as the concentration increases to the point where they cannot be distinguished from one another. This applies to both experiments. When both experiments are compared at lower concentrations ranging from 10-15%, the figures are similar. When the concentration is increased to 20%, a broader PSD is observed in the smooth bed experiments. This effect becomes even more evident at a concentration of 25%. However, when the concentration is increased above 25%, differences in PSD become difficult to distinguish as they become more and more similar, unlike the effects that were observed at a concentration of 20-25%

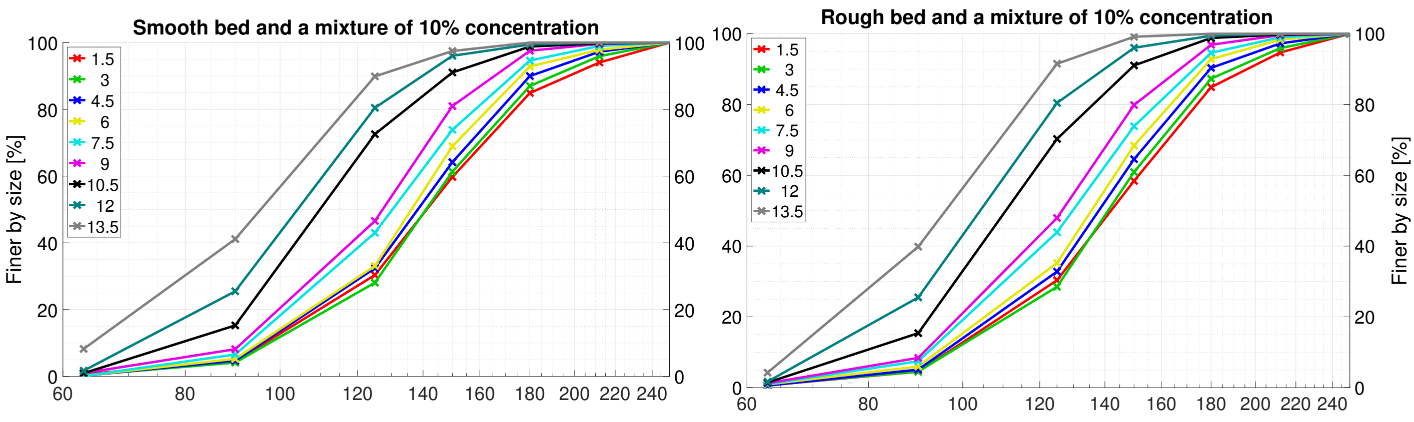

Figure 3.9: Particle size distribution of smooth and rough bed experiments.

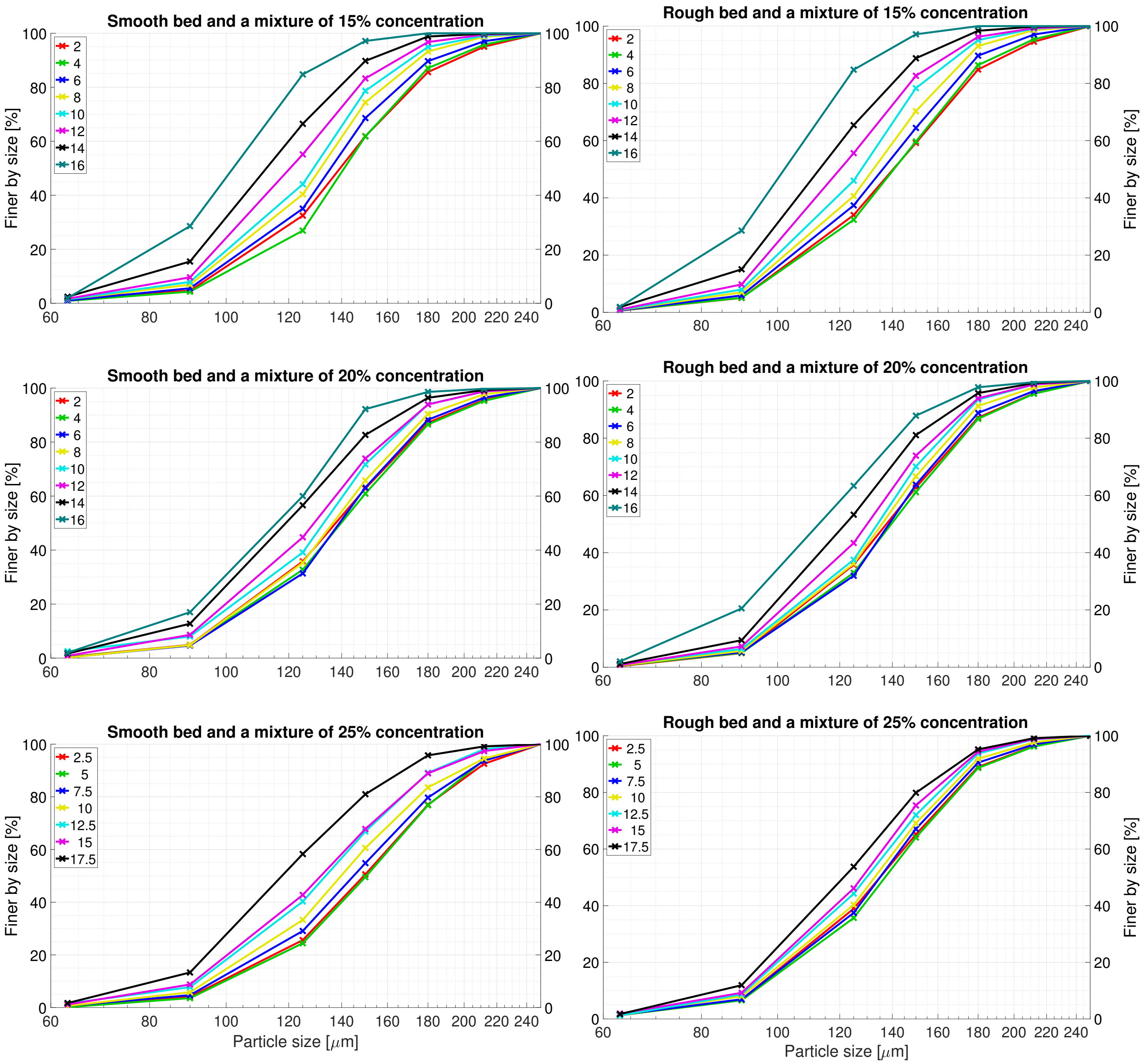

Figure 3.10: Particle size distribution of smooth and rough bed experiments.

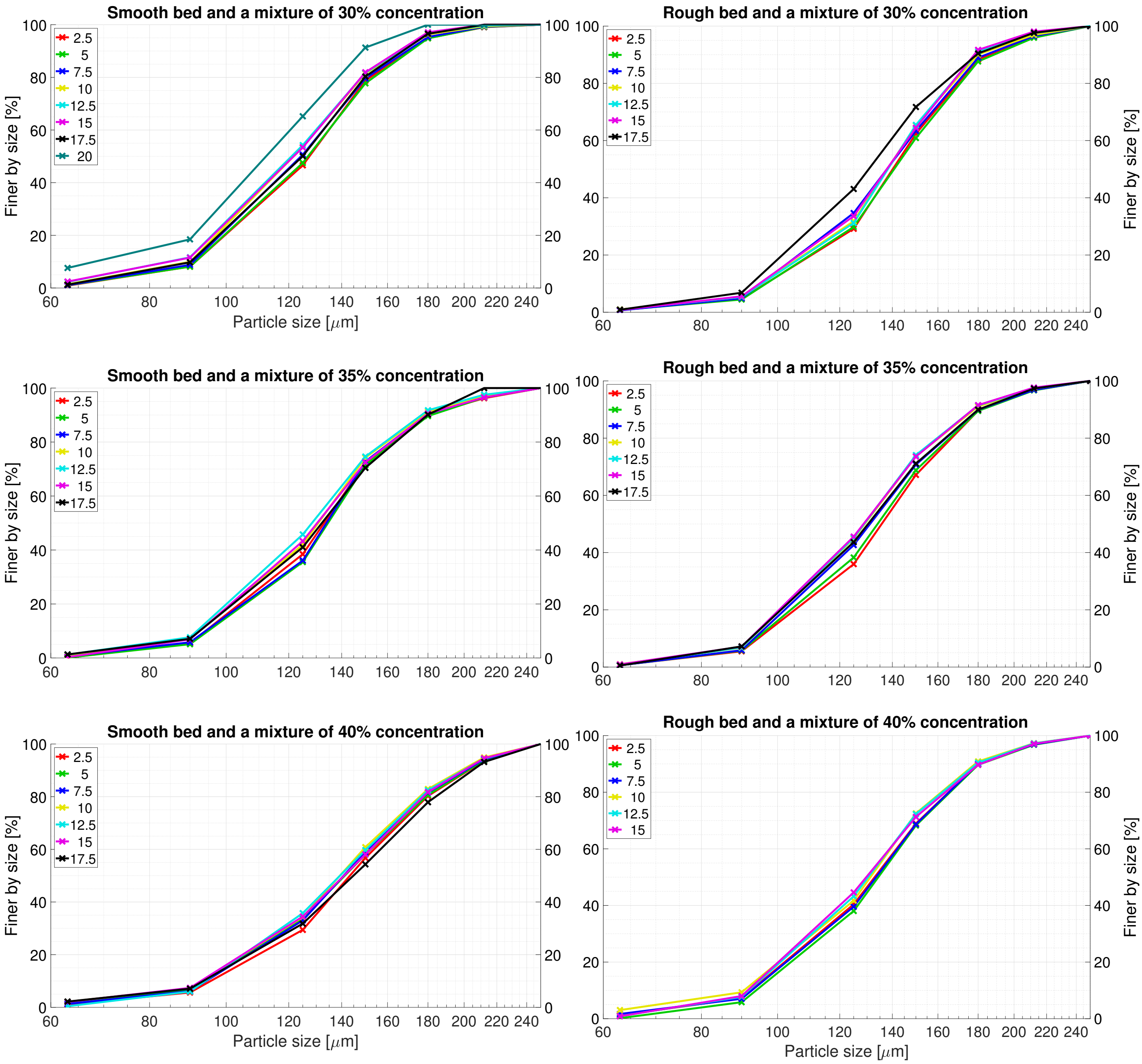

Figure 3.11: Particle size distribution of smooth and rough bed experiments.

3.3 Temperature

3.3.1 4 Phases

In figure 3.12, the results of experiments performed in warm and cold water can be observed. The cold water experiments are represented by the blue line in the graph and the warm water experiments are represented by the red line. The 4 phases, as seen earlier in the experiments performed over a smooth bed, can be distinguished in these experiments. This applies to both the warm- and cold water experiments at concentrations varying from 15% to 40% When the 4 phases are observed in the experiments with a difference in the water temperature, no difference is seen in phase 1 or phase 2 between the experiments regardless of concentration. The 3rd phase however, in contrast to phase 1 and 2, sets in earlier at both lower and higher concentrations in the warm-water experiments compared to the cold water experiments.

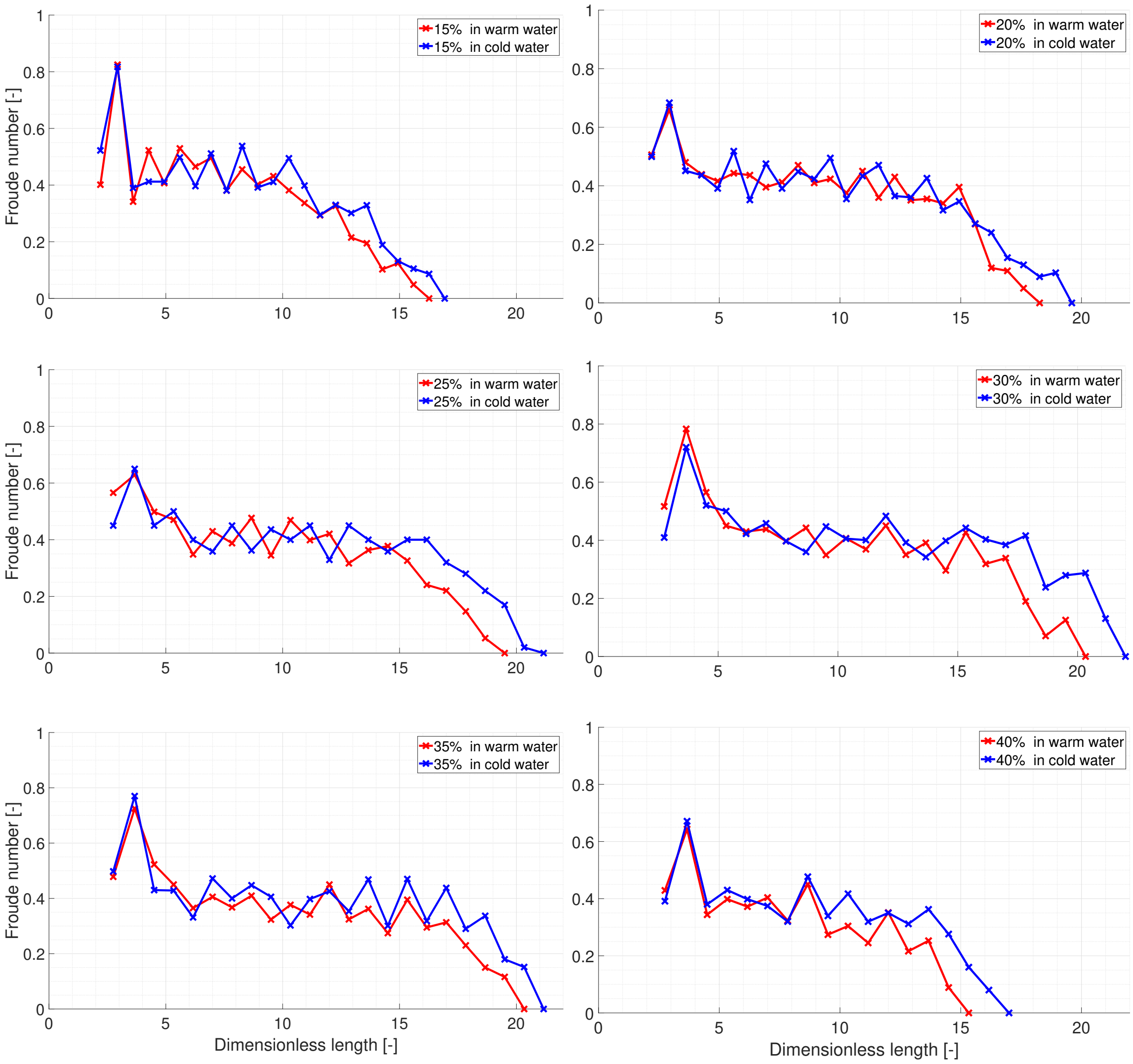

Figure 3.12: Four phases of cold and warm water experiments.

3.3.2 Run-out length

As can be seen clearly in table 3.2 , the run out-length of all experiments performed in warm water, is shorter in comparison to the cold-water experiments

Table 3.2: Run-out length in cold and warm water.

	Cold water	Warm water
15%	17,20	16,27
20%	18,80	17,73
25%	21,17	19,42
30%	22,08	20,33
35%	21,09	20,17
40%	17,06	15,42

3.3.3 Particle size distribution

The warm-water experiments are shown on the left side and the cold-water experiments are shown on the right side of figures 3.13 and 3.14. The experiments performed at a concentration varying from 15% to 25%, no great difference in PSD can be observed. When the concentration increases above 25% however, a denser PSD is observed in the cold-water experiments than in the warm-water experiments. The differences are subtle but noticeable.

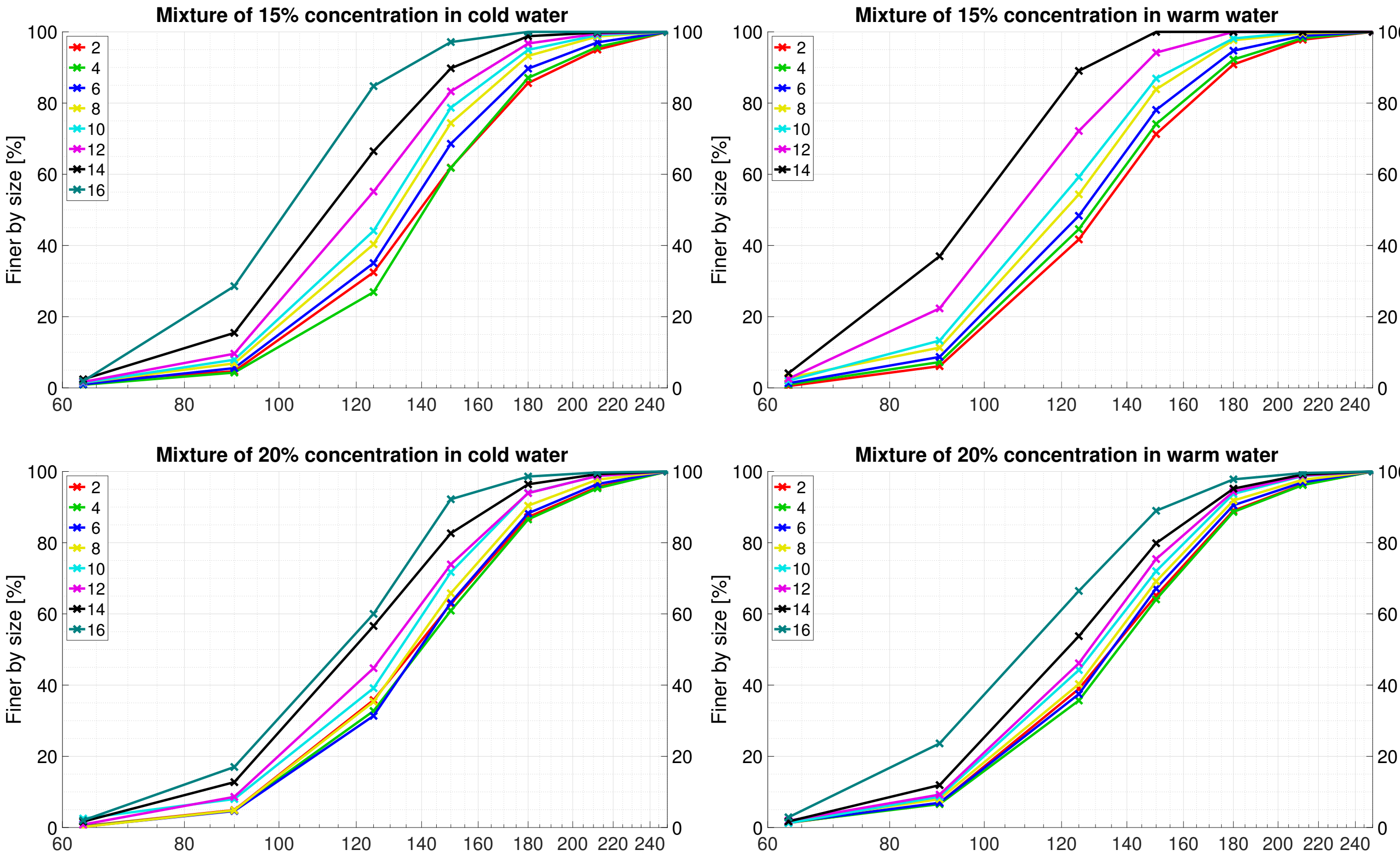

Figure 3.13: Particle size distribution of cold and warm water experiments.

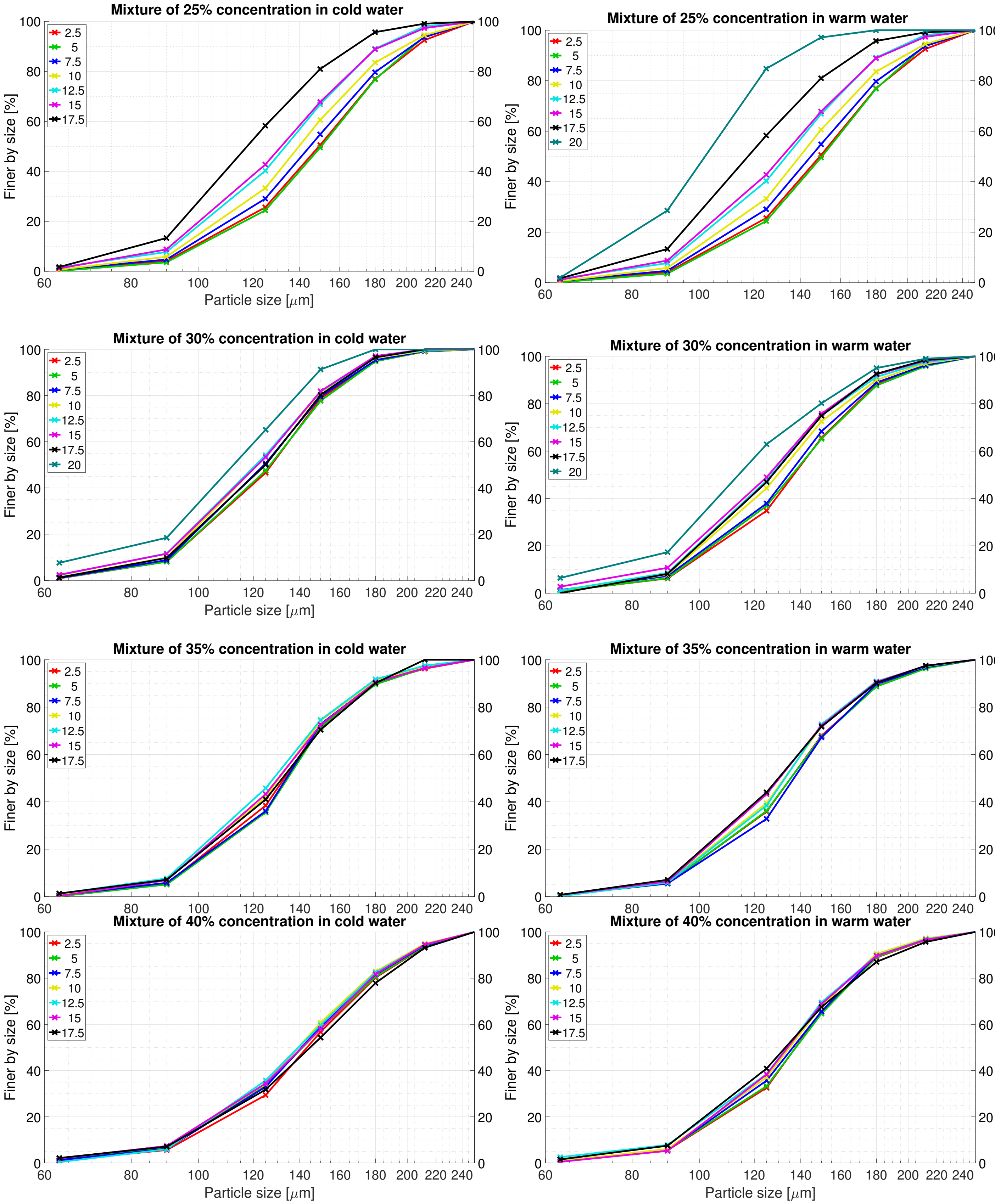

Figure 3.14: Particle size distribution of cold and warm water experiments.

Chapter 4

Numerical model verification

In this chapter, the experimental results are verified by means of a numerical model. Since there is no analytic solution for the two layer SW equations for a particle gravity current, the equations must be solved numerically. The numerical model is used to compare the outcome of the experimental results. The numerical model also helps to investigate the influence of particle size, bed roughness and temperature. In order to ease the comparison and reconstruct similar conditions as the experiments, the numerical model also uses the same approach as the experiments in chapter 3.

4.1 Influence of mono- and bi-dispersed mixtures

4.1.1 Mono-disperse mixture

A comparison was made between a current consisting of a mixture with an d50 of 138 μm versus a mono-dispersed current with an identical particle size (138 μm). As can be seen in figure 4.1, the figures have a similar development in the beginning, but as the currents progress/but in the stages following, it becomes evident that the mono-disperse currents settle before the poly-disperse currents do.

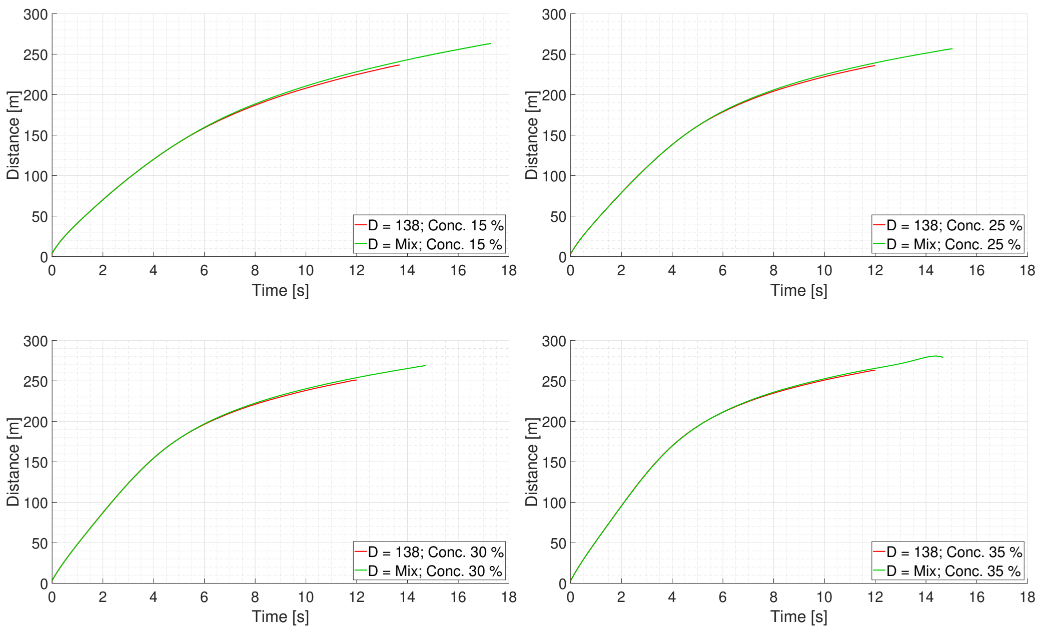

Figure 4.1: Influence of mixture type and concentration on run-out length.

4.1.2 Bi-disperse mixture

In figure 4.2 bi-dispersed experiments are displayed. These were performed to assess whether the model behaves in accordance to the observations that were made in the laboratory experiments. Different concentrations with a 50/50 ratio of several particle sizes were examined. In figure 4.2, it can be seen that the ratio is not 50/50 at the start of the measurement. When the concentration is increased, the ratio's start approaching the 50/50 distribution. In the end of each experiment, the small particle size takes over.

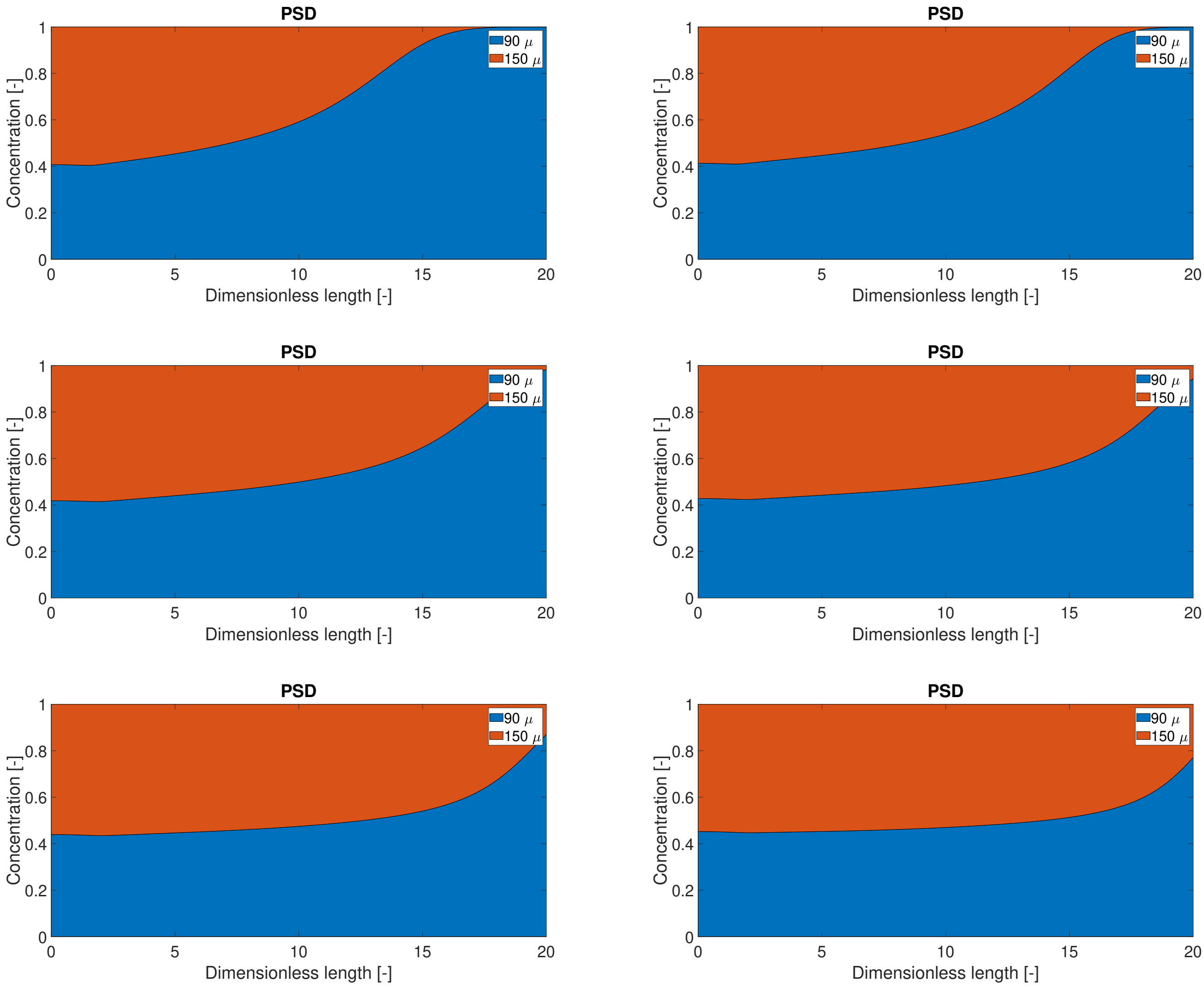

Figure 4.2: Influence of particle size on run-out length.

4.1.3 Mono Bi-disperse mixture

In figure 4.3, the results are displayed of the run out length of currents consisting of different mixtures and concentrations. What can clearly be observed is that the mixtures consisting of 90 μm particles have a longer run-out length at all concentrations while the 150μm particle mixtures have the shortest run-out length at all concentrations. Furthermore, the figures show that when both particle sizes are present in the mixture, the current has a longer run-out length at lower concentrations than at higher concentrations in comparison.

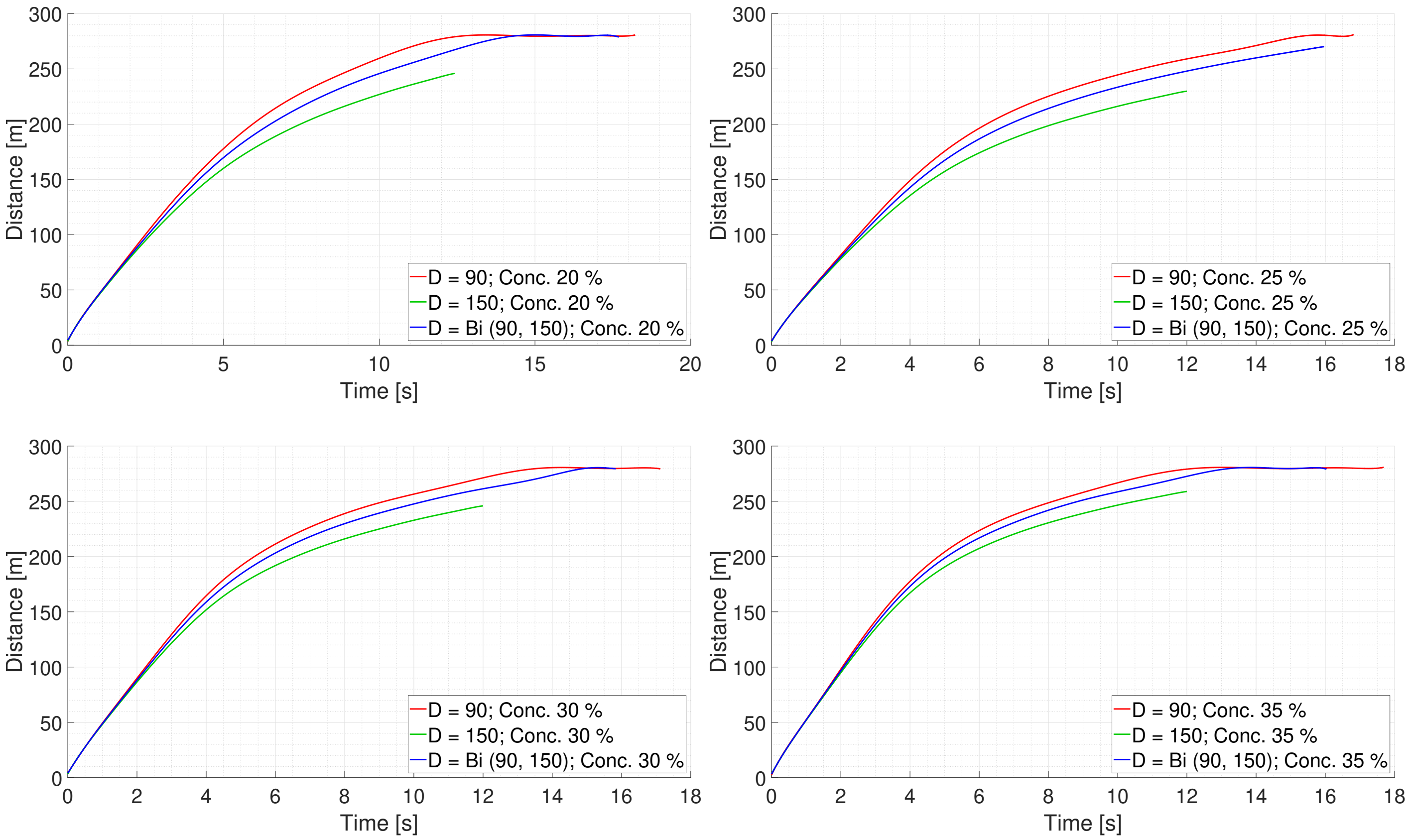

Figure 4.3: Influence of mixture type and concentration on run-out length.

4.2 Verification of Bed roughness

In figure 4.4, a comparison was made between the PSD of experiments performed at a concentration of 15% and 30%. Additionally, the friction coefficient was varied to analyse the influence of an increase in bed roughness. What stands out, is that an increase of the friction coefficient leads to a broadening of the PSD over the course of the run-out length

In figure 4.5, experiments performed with gravity currents with a concentration of 15% and 30%, are displayed. In these experiments, the influence of a friction increase from 0,011 to 0,2 on the gravity current gradients was analysed. The higher the friction coefficient, the slower the current and the shorter the run-out length, as can be observed in the figure. This applies to the gravity currents at both concentration.

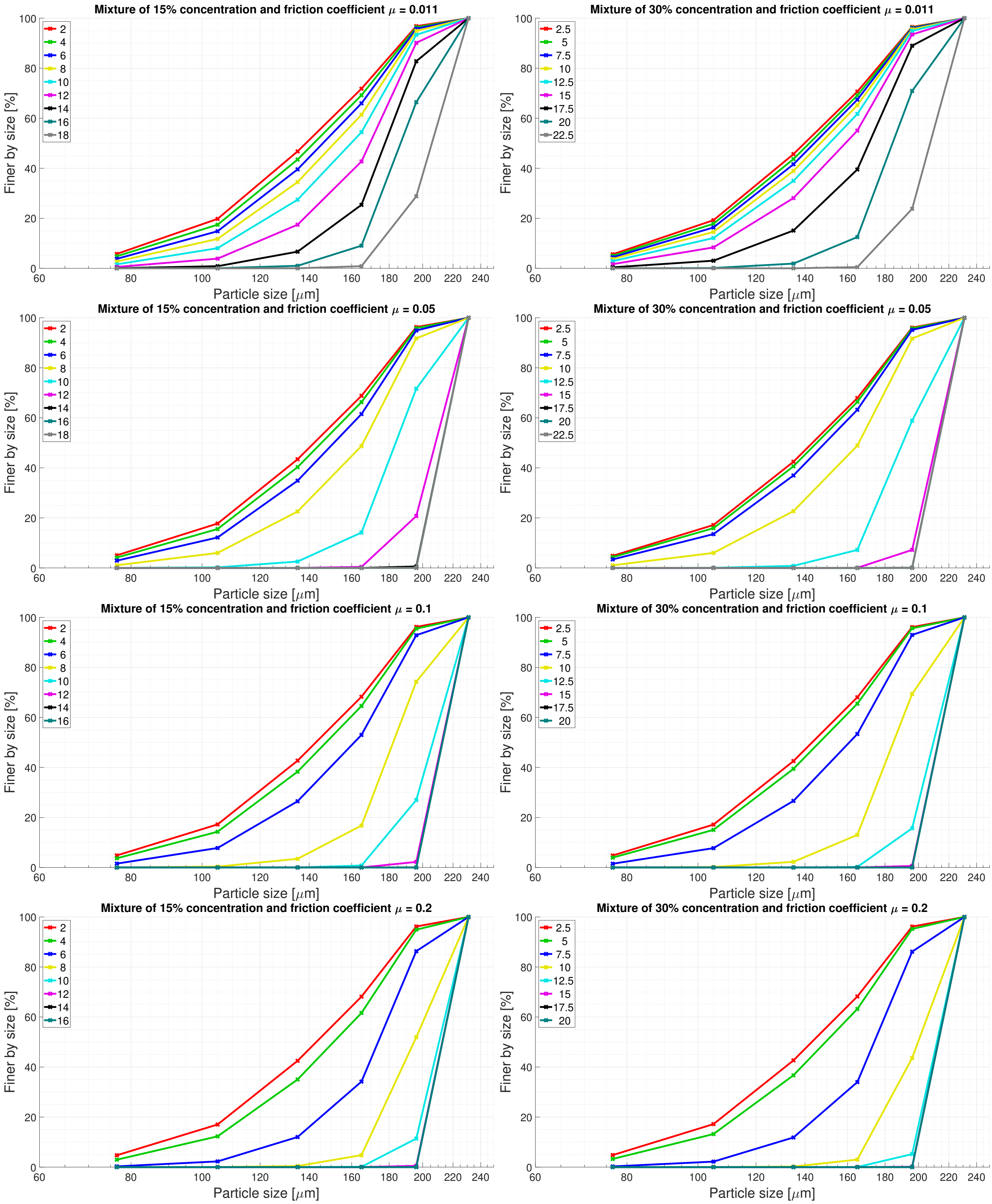

Figure 4.4: Influence of roughness on particle size distribution.

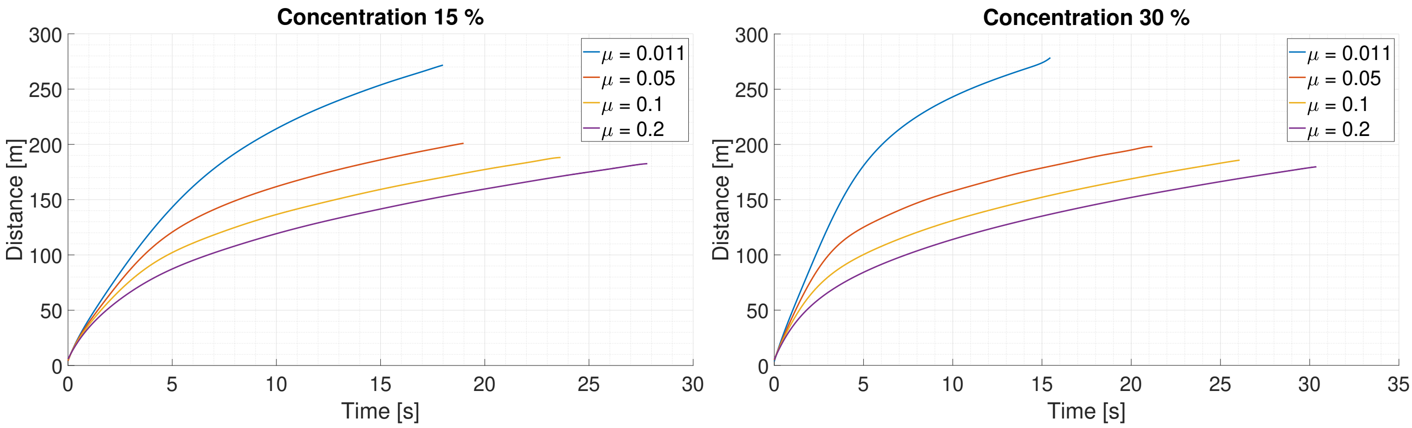

Figure 4.5: Influence of roughness on run-out length.

4.3 Verification of temperature

In the laboratory experiments, the temperature of the water was modified. The temperature in the model was modified similarly to assess if the results would resemble the results of the laboratory experiments, meaning that the model could accurately predict changes caused by temperature differences. In figure 4.7, the cold water experiments with different concentrations are displayed and these are compared to the warm water experiments shown on the right side of this figure. A difference in PSD can be observed in all experiments. The PSD in the cold water experiments are smaller than the PSD in the warm water experiments, as can be seen in the figure. Interesting differences can clearly be distinguished in the model regarding the cold- and warm water experiments.

The run-out length of both experiments are also assessed by the model. The results are displayed in figure 4.6. Again, the run-out length of the cold-water experiments is shorter compared to the run-out length of the warm water experiments.

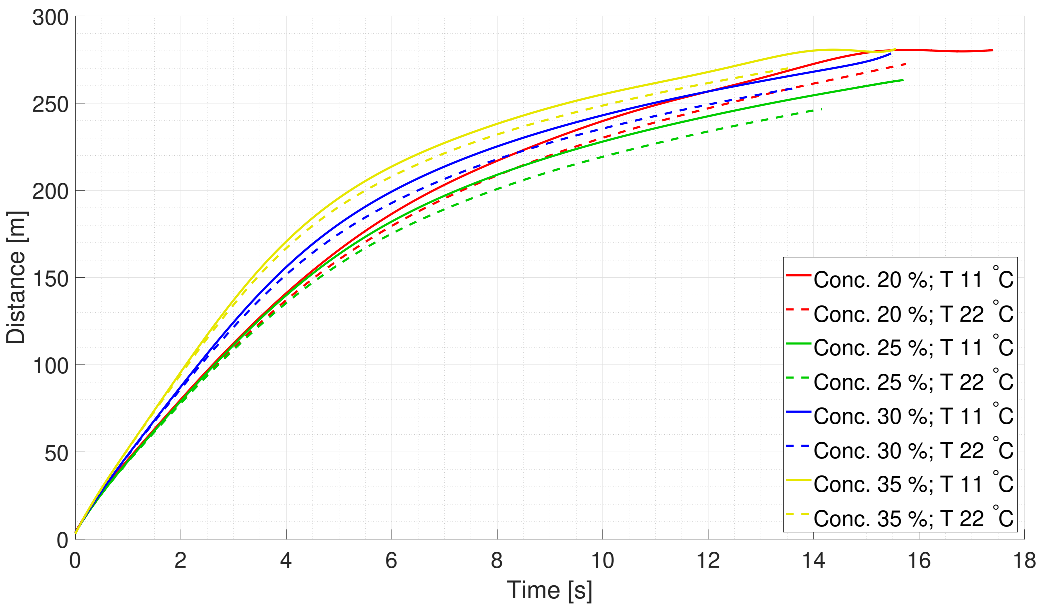

Figure 4.6: Influence of temperature on run-out length.

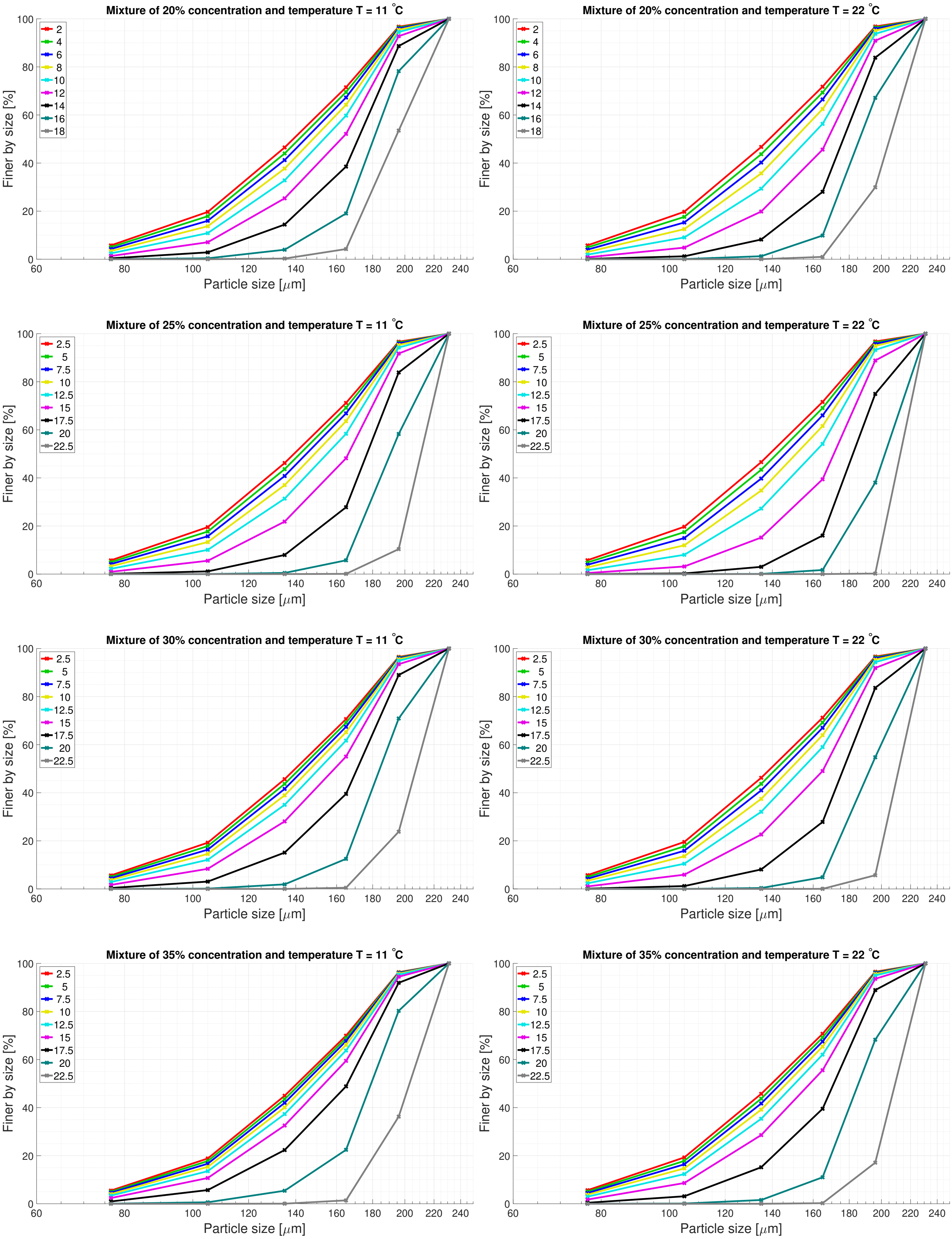

Figure 4.7: Influence of temperature on particle size distribution.

Chapter 5

Conclusions and recommendations

5.1 Conclusion

Based on the research done and the simulations performed the following conclusions are drawn.

5.1.1 Mono and bi-disperse mixtures

- The settling velocity of an individual particle can be calculated over a great variety of Reynolds numbers with the equation of [Ferguson and Church, 2004]. From this equation follows that the greater the particle size, the higher the settling velocity and thus the shorter the run-out length. This is in accordance with the results described in chapter 3. The formula shows that a decrease in particle size leads to a reduction of the settling velocity. This same phenomenon can be seen in the experiments performed with current consisting of particles with a diameter of 90 μm and currents consisting of particles with a diameter of 150 μm. The results of the experiments show that currents driven by 90 μm particles travel further than the ones driven by a 150 μm particle size, which translates to a longer run-out length for the 90 μm particle driven current. This is consistent with literature findings. It is described that mono-dispersed current consisting of smaller particle sizes with a low settling velocity have a longer run-out length than currents that consist of particles with a larger diameter and have a higher settling velocity.

- However, in nature, particles are not the same size. This means that natural gravity currents are multi particle currents. This makes the current development more complex. This has been researched by [Gladstone and Woods, 2000]. Some interesting findings from this article include that adding fine particles to the mixture of the current cause the run-out length of the current to increase. This is true even when only a small amount of fine particles are added, making up a low percentage of the total particles. This effect is also very noticeable when the concentration is increased in experiments with bi-disperse mixtures in order to compare the PSD. The following happens:
  - At low concentrations, a steep slope is visible because in the beginning of the experiment, the current consists mainly of larger particles. As the current evolves towards the end of the experiment, the ratio of small and large particles changes. The small particles outnumber the larger particles at the last stages of the experiment.
  - As the concentration is increased, the slope becomes horizontal. At higher concentrations, the ratio of smaller and larger particles is nearly identical.
  - When the concentration is increased to 30% or higher, the ratio of smaller and bigger particles becomes equivalent over the run out length.

- In the bi-disperse experiments conducted for this thesis, different concentrations were compared, while the ratio's were kept 50/50. All experiments show results consistent with the literature. The run-out length increases when smaller particles are added compared to experiments performed with only larger particles. Though, when the concentration is increased, an interesting effect can be observed. The influence of the smaller particles on the run-out length seems to decrease when the concentration is increased. This could be explained by the hindered settling effect which increases at higher concentrations. This shows the importance of the principal of hindered settling for the PSD of the gravity current.

5.1.2 Bed roughness

- Experiments were performed over a smooth- and a rough bed to investigate the influence of a rough bed. 14 different experiments were performed by varying the initial density of the particle mixture in the lock, maintaining all the other experimental variables constant. The experiments show that currents flowing over a rough bed travel less far than similar experiments over a smooth bed. This is in accordance with the literature, [La Rocca et al., 2008] found that the presence of a rough bed caused the current to travel less far at a lower velocity compared to experiments over a smooth bed.

- Another remarkable observation has not been covered in literature. The descriptions made in this thesis are based on the 4 phases model of the gravity current as described earlier. However, in the experiments performed over a rough bed at low concentrations, phase 1 cannot be distinguished. When the concentration is increased, phase 1 becomes visible again. Nonetheless, phase 1 remains lower compared to smooth bed experiments. A possible explanation could be that phase 1 is an acceleration that is caused by the opening of the lock. In a smooth bed experiment, the particles will not have trouble travelling contrary to particles that travel over a rough bottom. Travelling over a rough bed will be even more difficult at lower concentrations due to the reduced pressure.

- What is also worth noting, is that rough bed experiments have a smaller PSD compared to smooth bed experiments. What might explain this is that the rough bottom causes the particles to go back into the current instead of remaining on the bottom. In the literature, it is described that increased mixing occurs over rough beds, but this has been described in density current experiments, not in particle-driven currents.

5.1.3 Temperature

- What can be concluded from a Literature research on the influence of temperature is that at higher temperatures, particles settle faster. This can be explained by a change in the viscosity. Viscosity (η) can be defined as the resistance of a fluid to movement. Examples of fluids with a low viscosity, thus able to flow easily, are water and ethanol. Oil and honey on the contrary, are heavier fluids which move slowly, making them examples of high viscosity fluids. An important factor that can influence the viscosity is temperature. When temperature increases, the kinetic energy of the molecules increases as well. This as a result reduces the influence of attracting forces making it easier for the fluid to flow. So higher temperature leads to a lower viscosity in fluids which allows the fluids to flow more easily.

- In the experiments performed in cold and warm water, we can see that the particles in warm water settle faster than the particles in cold water. This is consistent with the literature. The same applies to the results of the numerical model. In this model, only the viscosity was adjusted to enable a comparison with the experiments that were performed at a temperature of 11 and 22 degrees Celsius.

- Another finding from our results is that the PSD is denser in experiments performed in cold water. This difference is also apparent in the numerical model. An explanation for this finding can be given by focusing on the viscosity. When the viscosity decreases, the particle settlement will increase. Therefore, the current will settle entirely at a faster pace. Smaller particles will settle faster than larger particles, resulting in a broader PSD. The opposite applies to an increase of the viscosity. At lower temperatures, the viscosity increases, leading to slower settlement of both smaller and larger particles, which in turn will result in a smaller PSD. From these findings, we can conclude that an increase in temperature can cause the current to travel less far and leads to a broader PSD when compared to cold water experiments.

5.2 Recommendations

5.2.1 Mono and bi-disperse mixtures

- To get more insight in the effect of the particle sizes in the currents, it would be highly recommended to conduct more experiments with a greater difference between particle sizes. This would allow for a better assessment of the magnitude of the effect of hindered settling.

5.2.2 Bed roughness

- To gain a better understanding of this subject, it is vital to perform different experiments to observe what exactly takes place in the current development and how the rough bed influences this process. It would be advisable to experiment with gravity currents over rough beds of different diameters. To improve the model and to give the right value of the friction coefficient to certain rough beds, natural gravity currents travelling over rough beds should be observed and recreated in the model to find a corresponding friction coefficient which could then be used in the future to accurately predict the influence of rough beds on the behaviour of gravity currents.

5.2.3 Temperature

- Temperature should be taken into account for modelling gravity currents. Otherwise this can lead to an overestimation regarding the run-out length and an underestimation of the deposit density.

Bibliography

[Bonnecaze et al., 1993] Bonnecaze, R. T., Huppert, H. E., and Lister, J. R. (1993). Particle-driven gravity currents. *Journal of Fluid Mechanics*, 250:339–369.

[Dade and Huppert, 1995] Dade, W. B. and Huppert, H. E. (1995). A box model for non-entraining, suspension-driven gravity surges on horizontal surfaces. *Sedimentology*, 42(3):453–470.

[Ferguson and Church, 2004] Ferguson, R. and Church, M. (2004). A simple universal equation for grain settling velocity. *Journal of sedimentary Research*, 74(6):933–937.

[Gladstone and Woods, 2000] Gladstone, C. and Woods, A. W. (2000). On the application of box models to particle-driven gravity currents. *Journal of fluid mechanics*, 416:187–195.

[Hallworth and Huppert, 1998] Hallworth, M. A. and Huppert, H. E. (1998). Abrupt transitions in high-concentration, particle-driven gravity currents. *Physics of Fluids*, 10(5):1083–1087.

[Hallworth et al., 1996] Hallworth, M. A., Huppert, H. E., Phillips, J. C., and Sparks, R. S. J. (1996). Entrainment into two-dimensional and axisymmetric turbulent gravity currents. *Journal of Fluid Mechanics*, 308:289–311.

[Harris et al., 2001] Harris, T. C., Hogg, A. J., and Huppert, H. E. (2001). A mathematical framework for the analysis of particle–driven gravity currents. *Proceedings of the Royal Society of London. Series A: Mathematical, Physical and Engineering Sciences*, 457(2009):1241–1272.

[Huppert and Simpson, 1980] Huppert, H. E. and Simpson, J. E. (1980). The slumping of gravity currents. *Journal of Fluid Mechanics*, 99(4):785–799.

[La Rocca et al., 2008] La Rocca, M., Adduce, C., Sciortino, G., and Pinzon, A. B. (2008). Experimental and numerical simulation of three-dimensional gravity currents on smooth and rough bottom. *Physics of Fluids*, 20(10):106603.

[Necker et al., 2005] Necker, F., Härtel, C., Kleiser, L., and Meiburg, E. (2005). Mixing and dissipation in particle-driven gravity currents. *Journal of Fluid Mechanics*, 545:339.

[Peters and Venart, 2000] Peters, W. D. and Venart, J. (2000). Visualization of rough-surface gravity current flows using laser-induced fluorescence. In *9th (Millennium) International Symposium on Flow Visualization*.

[Rottman and Simpson, 1983] Rottman, J. W. and Simpson, J. E. (1983). Gravity currents produced by instantaneous releases of a heavy fluid in a rectangular channel. *Journal of Fluid Mechanics*, 135:95–110.

[Shin et al., 2004] Shin, J., Dalziel, S., and Linden, P. (2004). Gravity currents produced by lock exchange. *Journal of Fluid Mechanics*, 521:1–34.

[Stovers, 2016] Stovers, M. (2016). Particle-driven gravity currents.

[Thomas, 1965] Thomas, D. G. (1965). Transport characteristics of suspension: Viii. a note on the viscosity of newtonian suspensions of uniform spherical particles. *Journal of Colloid Science*, 20(3):267–277.

[Zhu et al., 2006] Zhu, J. B., Lee, C. B., Chen, G. Q., and Lee, J. H. W. (2006). Piv observation of instantaneous velocity structure of lock release gravity currents in the slumping phase. *Communications in Nonlinear Science and Numerical Simulation*, 11(2):262–270.

Appendix A

Sieve curve

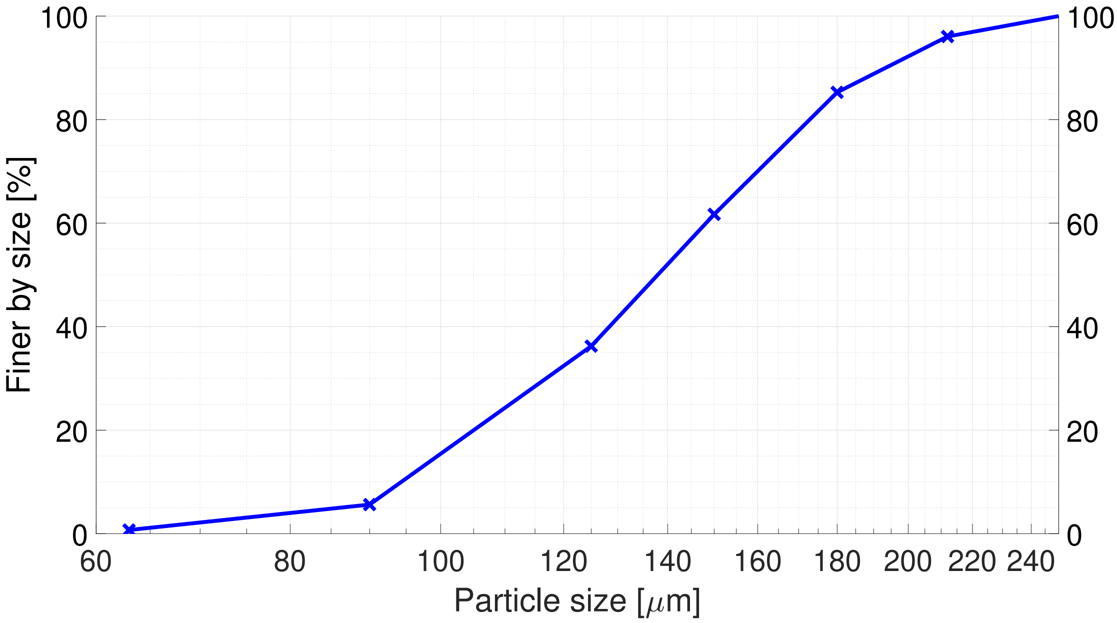

Figure A.1: Sieve curve Geba weis sand.